NASA Contractor Report 181964
ICASE Report No. 89–44

ICASE

BOUNDARY ESTIMATION PROBLEMS ARISING IN THERMAL TOMOGRAPHY

H. T. Banks
Fumio Kojima
W. P. Winfree

Contract No. NAS1–18605
November 1989

Institute for Computer Applications in Science and Engineering
NASA Langley Research Center
Hampton, Virginia 23665–5225

Operated by the Universities Space Research Association

National Aeronautics and
Space Administration

Langley Research Center
Hampton, Virginia 23665-5225

BOUNDARY ESTIMATION PROBLEMS ARISING IN THERMAL TOMOGRAPHY *

H. T. Banks
Center for Applied Mathematical Sciences
University of Southern California
Los Angeles, CA 90089-1113

Fumio Kojima
Institute for Computer Applications in Science and Engineering
NASA Langley Research Center
Hampton, VA 23665

W. P. Winfree
Instrument Research Division
NASA Langley Research Center
Hampton, VA 23665

ABSTRACT

Problems on the identification of two dimensional spatial domains arising in the detection and characterization of structural flaws in materials are considered. For a thermal diffusion system with external boundary input, observations of the temperature on the surface are used in a output least square approach. Parameter estimation techniques based on the "method of mappings" are discussed and approximation schemes are developed based on a finite element Galerkin approach. Theoretical convergence results for computational techniques are given and the results are applied to experimental data for the identification of flaws in thermal testing of materials.

*This research was carried out in part while the first and second authors were in residence at the Institute for Computer Applications in Science and Engineering (ICASE), NASA Langley Research Center, Hampton, VA 23665, which is operated under NASA Contract No. NAS1-18605. Additional support for the first author was also provided by the National Science Foundation under NSF Grant No. DMS-8818530 and by the Air Force Office of Scientific Research under contract F49620-86-C-0111.

I. INTRODUCTION

Domain identification problems are important in engineering design and frequently, such problems are treated as a branch of the calculus of variations. Discussions usually involve nonlinear optimization techniques, optimal control theory, partial differential equations and related numerical algorithms. Domain identification for elliptic systems has been studied theoretically and numerically by many authors (for example, see [5], [8],[16], [17],[18]). Most efforts have been concentrated on problems of optimal shape design which are motivated by numerous applications to structural, airplane, ship design, etc. (see [17] and the references therein). In this paper, our concern for domain identification is motivated by an application that differs somewhat from these shape design problems. Recently, in space structures studies, fiber reinforced composite materials have been widely proposed and, as a result, demand has grown for assessing the structural integrity of structures made from these materials. An important effort on such problems entails non-destructive evaluation methods in thermal tomography. These methods involve an attempt to characterize structural flaws (e. g., corrosion, cracks, etc.) which may not be detectable by visual inspection (see [9] for more details). Mathematically, these problems can be treated as domain identification problems. Initial efforts by the authors on the inverse problems of 2-D thermal tomography were detailed in [3], [4]. In this paper, we present a more general version of the ideas proposed in [3], [4] by using the "method of mappings" (see [16], [17]). Moreover, we report on the successful use of the proposed method with both noisy simulated data and experimental data from material studies in the Nondestructive Measurement Science Branch at NASA Langley Research Center. Other studies closely related to our work have been discussed in [9] and [10].

To explain our approach, we focus our attention on a 2-D domain identification problem. We consider a bounded domain G in two-dimensional Eucledean space as depicted in Fig. 1. Let Γ (the region of corrosion) be the section of the boundary where the detection of structural flaws is to be attempted via identification of Γ. We assume that the boundary of

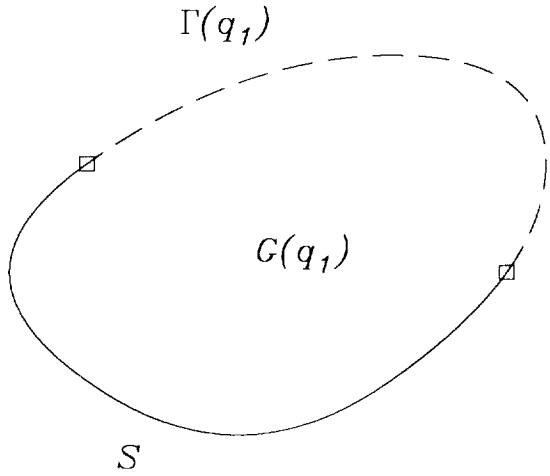

Figure 1. Spatial domain $G(q)$ bounded by $S \bigcap \Gamma(q)$.

G is decomposed into two parts $\partial G = S \cup \Gamma$, where S is the known surface of the material. The system behavior is governed by the 2-D diffusion equation,

$$\frac{\partial u}{\partial t} - c\Delta u = 0 \quad \text{in } \mathcal{T} \times G \tag{1}$$

with the initial and boundary conditions

$$u(t_0) = \overline{u}_0 \quad \text{on } G \tag{2}$$

$$c\frac{\partial u}{\partial n} = f \quad \text{on } \mathcal{T} \times S \tag{3}$$

$$\frac{\partial u}{\partial n} = 0 \quad \text{on } \mathcal{T} \times \Gamma \tag{4}$$

where c is a given constant representing the thermal diffusivity and where $\mathcal{T}$ denotes the time interval (t_0, t_f) during which the process is observed. In general, the external boundary input f can not be measured directly and must also be estimated. For our efforts here we parametrize the flux f as a function of an n_0-dimensional vector q_0, i. e.,

$$f = f(q_0).$$

We further assume that the corrosion shape at the unknown section Γ of the boundary is specified by an n_1-dimensional parameter vector q_1,

$$\Gamma = \Gamma(q_1).$$

The system domain $G = G(q_1)$ is bounded by the partially unknown boundary $S \cup \Gamma(q_1)$. In treating experimental data, it is often necessary to estimate the initial data from boundary observations at time t_0. The resulting estimate will be dependent on $q = (q_0, q_1)$ through both the domain and the input flux. Hence in our presentation the initial state function is set as

$$\overline{u}_0 = \overline{u}_0(q).$$

The system output (i. e. the observations of the temperature) is assumed to be on a subset Σ of S and, mathematically, the observation is taken as

$$y(t, q) = u(t, q)|_{\Sigma}. \tag{5}$$

The problem treated theoretically and computationally in this paper is that of identifying, from output data $\{y\}$, the constant parameter vector q determining the geometrical structure of the domain $G(q_1)$ and the boundary input function $f(q_0)$. Let $q = (q_0, q_1)$ be a constant parametrization vector among values in a given parameter set Q. Throughout this paper, we assume that

(H-0) The admissible parameter set $Q = Q_0 \times Q_1$ is a compact subset of $R^{n_0} \times R^{n_1}$.

II. DOMAIN IDENTIFICATION BY THE METHOD OF MAPPINGS

We consider a reference domain C which is a bounded open set in R^2. The reference domain C is taken in the same topology as that of $G(q_1)$. Moreover, the domain C is bounded by a smooth boundary ∂C. Then, we introduce the bijective mapping $T(q_1)$ from C into $G(q_1)$,

$$x = T(q_1) \circ z$$

as depicted in Fig. 2. Mathematically, we make the hypotheses for the mapping $T(q_1)$ as follows:

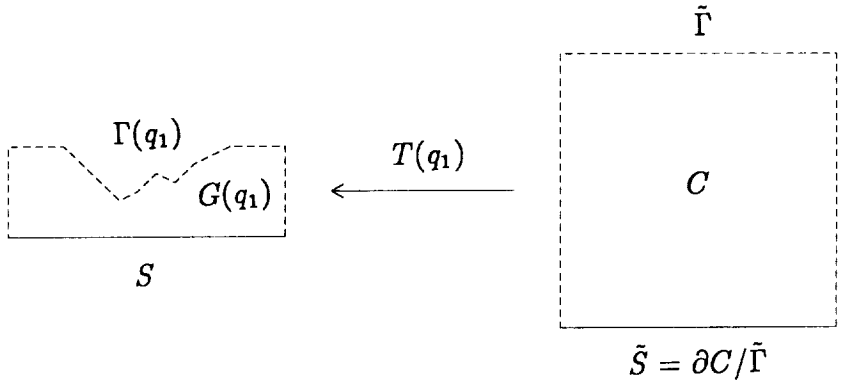

Figure 2. Transformation mapping from C into $G(q_1)$.

(H-1) The unknown domain $G(q_1)$ is given by

$$G(q_1) = T(q_1)(C)$$

with existence of $\tilde{\Gamma} \subset \partial C$ such that $\tilde{S} \equiv \partial C/\tilde{\Gamma} = S$ and

$$\Gamma(q_1) = T(q_1)(\tilde{\Gamma}), \qquad S = T(q_1)(\tilde{S}) = \tilde{S}$$

where S is independent of q_1.

If we consider a variational formulation similar to that in [13], the system dynamics (1) - (4) can be described by

$$\int_{G(q_1)} \{\frac{du}{dt}\phi + c\nabla u \cdot \nabla\phi\} dx = \int_S f(q_0)(\gamma_S \phi) d\xi_S \quad \text{for} \quad \text{all } \phi \in H^1(G(q_1)) \tag{6}$$

with

$$u(t_0) = \overline{u}_0(q), \tag{7}$$

where γ_S denotes the trace operator on S and $d\xi_S$ is a line element on the boundary curve S. Using the mapping $T(q_1)$, we may obtain the variational formulation defined on the reference domain C.

Proposition 1: Define

$$\tilde{u}(t) = u(t) \circ T(q_1).$$

Then the transformed system dynamics can be described by

$$< \frac{d\tilde{u}}{dt}, \phi >_{L^2(C)} + \sigma(q_1)(\tilde{u}(t), \phi) = L(q)(\phi) \quad \text{for all } \phi \in H^1(C) \tag{8}$$

with

$$\tilde{u}(t_0) = \overline{u}_0(q) \circ T(q_1) \quad (\stackrel{def}{=} \tilde{u}_0(q)) \tag{9}$$

where $\sigma(q_1)(\cdot,\cdot)$ and $L(q)(\cdot)$ denote, respectively, a sesquilinear form on $H^1(C) \times H^1(C)$ and a linear form on $H^1(C)$ such that, for $\phi, \psi \in H^1(C)$

$$\begin{aligned} \sigma(q_1)(\phi,\psi) \stackrel{def}{=} & \int_C [c\nabla\phi \cdot (\nabla T(q_1))^{-t}(\nabla T(q_1))^{-1}\nabla\psi \\ & -c\nabla\phi \cdot \{\det(\nabla T(q_1))\}^{-1}(\nabla T(q_1))^{-t}(\nabla T(q_1))^{-1}\{\nabla \det(\nabla T(q_1))\}\psi]dz \end{aligned} \tag{10}$$

$$L(q)(\phi) \stackrel{def}{=} \int_S f(q_0)(\gamma_S\phi)\left[\gamma_S\{\det(\nabla T(q_1))\}^{-1}\right] d\xi_S \tag{11}$$

respectively.

Proof: The weak formulation of (6) can be transformed into

$$\begin{aligned} & \int_C \left[\frac{d\tilde{u}}{dt}\tilde{\phi} + c\nabla\tilde{u} \cdot (\nabla T(q_1))^{-t}(\nabla T(q_1))^{-1}\nabla\tilde{\phi}\right] \det(\nabla T(q_1))dz \\ & \qquad = \int_S f(q_0)(\gamma_S\tilde{\phi})d\xi_S \qquad \text{for} \quad \tilde{\phi} \in H^1(C). \end{aligned}$$

Setting $\tilde{\phi} = (\det(\nabla T(q_1)))^{-1}\phi$, we have

$$\begin{aligned} \int_C \frac{d\tilde{u}}{dt}\phi dz \; + \; & \int_C [c\nabla\tilde{u} \cdot (\nabla T(q_1))^{-t}(\nabla T(q_1))^{-1}\nabla\phi \\ - \; & c\nabla\tilde{u} \cdot \{\det(\nabla T(q_1))\}^{-1}(\nabla T(q_1))^{-t}(\nabla T(q_1))^{-1}\{\nabla \det(\nabla T(q_1))\}\phi]dz \\ & = \int_S f(q_0)(\gamma_S\phi)\left[\gamma_S\{\det(\nabla T(q_1))\}^{-1}\right] d\xi_S \end{aligned}$$

from which the representation (8) follows directly.

With some tedious calculations, one can readily establish the following useful conditions on the sesquilinear form σ.

Theorem 1: *Suppose that the mapping $T(q_1)$ satisfies the conditions*:

(C-1) *For each $q_1 \in Q_1$, we have*

$$T(q_1) \in W^1_\infty(\overline{C}) \times W^1_\infty(\overline{C})$$

$$\det(\nabla T(q_1)) \in W^1_\infty(\overline{C});$$

(C-2) *There exists a constant δ independent of q_1 such that, for each $q_1 \in Q_1$,*

$$\det(\nabla T(q_1)) \geq \delta > 0;$$

(C-3) *There exists a constant K_1 independent of q_1 such that, for each $q_1, \tilde{q}_1 \in Q_1$,*

$$|T(q_1) - T(\tilde{q}_1)|_{W^1_\infty(\overline{C})\times W^1_\infty(\overline{C})} \leq K_1 |q_1 - \tilde{q}_1|,$$

$$|\det(\nabla T(q_1)) - \det(\nabla T(\tilde{q}_1))|_{W^1_\infty(\overline{C})} \leq K_1 |q_1 - \tilde{q}_1|.$$

Then, the sesquilinear form $\sigma(q_1)(\cdot,\cdot)$ satisfies the following inequalities: There exist positive constants $\alpha, \lambda, \beta, \mu$ such that, for $\phi, \psi \in H^1(C)$, we have

$$\sigma(q_1)(\phi,\phi) \geq \alpha|\phi|^2_{H^1(C)} - \lambda|\phi|^2_{L^2(C)} \tag{12}$$

$$|\sigma(q_1)(\phi,\psi)| \leq \beta|\phi|_{H^1(C)}|\psi|_{H^1(C)} \tag{13}$$

$$|\sigma(q_1)(\phi,\psi) - \sigma(\tilde{q}_1)(\phi,\psi)| \leq \mu|q_1 - \tilde{q}_1|\,|\phi|_{H^1(C)}|\psi|_{H^1(C)}. \tag{14}$$

Proof: For convenience in discussions, the explicit form of the mapping $x = T(q_1)z$ is assumed to be given by

$$\begin{cases} x_1 = \psi_1(z, q_1) \\ x_2 = \psi_2(z, q_1) \end{cases}. \tag{15}$$

Noting that

$$\nabla T(q_1) = \begin{bmatrix} \frac{\partial \psi_1}{\partial z_1}(q_1) & \frac{\partial \psi_2}{\partial z_1}(q_1) \\ \frac{\partial \psi_1}{\partial z_2}(q_1) & \frac{\partial \psi_2}{\partial z_2}(q_1) \end{bmatrix},$$

we obtain

$$(\nabla T(q_1))^{-t}(\nabla T(q_1))^{-1} = \{\det(\nabla T(q_1))\}^{-2}$$
$$\times \begin{bmatrix} (\frac{\partial \psi_2}{\partial z_2}(q_1))^2 + (\frac{\partial \psi_1}{\partial z_2}(q_1))^2 & -\left\{\frac{\partial \psi_1}{\partial z_1}(q_1)\frac{\partial \psi_1}{\partial z_2}(q_1) + \frac{\partial \psi_2}{\partial z_1}(q_1)\frac{\partial \psi_2}{\partial z_2}(q_1)\right\} \\ -\left\{\frac{\partial \psi_1}{\partial z_1}(q_1)\frac{\partial \psi_1}{\partial z_2}(q_1) + \frac{\partial \psi_2}{\partial z_1}(q_1)\frac{\partial \psi_2}{\partial z_2}(q_1)\right\} & (\frac{\partial \psi_2}{\partial z_1}(q_1))^2 + (\frac{\partial \psi_1}{\partial z_1}(q_1))^2 \end{bmatrix}.$$

For economy of notation, we define the functions

$$\begin{aligned}
a_{11}(z,q_1) &= \left\{(\frac{\partial \psi_2}{\partial z_2}(q_1)\right\}^2 + \left\{\frac{\partial \psi_1}{\partial z_2}(q_1)\right\}^2 \\
a_{12}(z,q_1) &= a_{21}(z,q_1) \\
&= -\left\{\frac{\partial \psi_1}{\partial z_1}(q_1)\frac{\partial \psi_1}{\partial z_2}(q_1) + \frac{\partial \psi_2}{\partial z_1}(q_1)\frac{\partial \psi_2}{\partial z_2}(q_1)\right\} \\
a_{22}(z,q_1) &= \left\{\frac{\partial \psi_2}{\partial z_1}(q_1)\right\}^2 + \left\{\frac{\partial \psi_1}{\partial z_1}(q_1)\right\}^2 \\
b_1(z,q_1) &= -a_{11}(z,q_1)\frac{\partial}{\partial z_1}\{\det(\nabla T(q_1))\} - a_{12}(z,q_1)\frac{\partial}{\partial z_2}\{\det(\nabla T(q_1))\} \\
b_2(z,q_1) &= -a_{21}(z,q_1)\frac{\partial}{\partial z_1}\{\det(\nabla T(q_1))\} - a_{22}(z,q_1)\frac{\partial}{\partial z_2}\{\det(\nabla T(q_1))\}.
\end{aligned}$$

Then the sesquilinear form (10) can be rewritten as

$$\begin{aligned}
\sigma(q_1)(\phi_1,\phi_2) &= \int_C [c\{\det(\nabla T(q_1))\}^{-2} \sum_{i,j\le 2} a_{ij}(z,q_1)\frac{\partial \phi_1}{\partial z_j}\frac{\partial \phi_2}{\partial z_i} \\
&\quad + c\{\det(\nabla T(q_1))\}^{-3} \sum_{j\le 2} b_j(z,q_1)\frac{\partial \phi_1}{\partial z_j}\phi_2]dz. \qquad (16)
\end{aligned}$$

The principal part of the differential operator becomes

$$\begin{aligned}
&c\{\det(\nabla T(q_1))\}^{-2} \sum_{i,j\le 2} a_{ij}(z,q_1)\zeta_i\zeta_j = \\
&\quad c\{\det(\nabla T(q_1)\}^{-2} \left[\left\{\left(\frac{\partial \psi_2}{\partial z_2}(q_1)\right)^2 + \left(\frac{\partial \psi_1}{\partial z_2}(q_1)\right)^2\right\}\zeta_1^2\right. \\
&\quad -2\left\{\frac{\partial \psi_1}{\partial z_1}(q_1)\frac{\partial \psi_1}{\partial z_2}(q_1) + \frac{\partial \psi_2}{\partial z_1}(q_1)\frac{\partial \psi_2}{\partial z_2}(q_1)\right\}\zeta_1\zeta_2 \\
&\quad \left. + \left\{\left(\frac{\partial \psi_2}{\partial z_1}(q_1)\right)^2 + \left(\frac{\partial \psi_1}{\partial z_1}(q_1)\right)^2\right\}\zeta_2^2\right] \qquad \text{for} \quad \zeta = (\zeta_1,\zeta_2) \in R^2. \qquad (17)
\end{aligned}$$

This has the lower bound

$$\frac{c}{2}\min\left\{\frac{1}{a_{11}(z,q_1)},\quad \frac{1}{a_{22}(z,q_1)}\right\}|\zeta|^2.$$

Under the condition (C-1), there exists a constant R such that

$$|\psi_i| < R \qquad \left|\frac{\partial\psi_i}{\partial z_j}\right| < R \qquad \text{for} \quad i,j=1,2. \tag{18}$$

Hence we obtain

$$c\{\det(\nabla T(q_1))\}^{-2}\sum_{i,j\le 2} a_{ij}(z,q_1)\zeta_i\zeta_j \ge \frac{c}{4R^2}|\zeta|^2 > 0 \qquad \text{for} \quad \zeta\in R^2, \tag{19}$$

which means the operator is strongly elliptic. For the second term in (16), it follows that

$$\left|c\{\det(\nabla T(q_1))\}^{-3}\sum_{j\le 2} b_j(z,q_1)\frac{\partial\phi_1}{\partial z_j}\phi_2\right|$$

$$\le c\,|\det(\nabla T(q_1))|^{-3}\left\{|b_1(z,q_1)|\left|\frac{\partial\phi_1}{\partial z_1}\right| + |b_2(z,q_1)|\left|\frac{\partial\phi_1}{\partial z_2}\right|\right\}|\phi_2|.$$

Under (C-1), we note that R can be chosen so that we also have

$$|\det(\nabla T(q_1))| < R$$

$$\left|\frac{\partial}{\partial z_i}\{\det(\nabla T(q_1))\}\right| < R \qquad \text{for} \quad i=1,2. \tag{20}$$

From (18) and (20), we obtain

$$|b_j(z,q_1)| < 4R^3 \qquad \text{for} \quad j=1,2.$$

Hence, by virtue of (C-2), it follows that

$$\left|c\{\det(\nabla T(q_1))\}^{-3}\sum_{j\le 2} b_j(z,q_1)\frac{\partial\phi_1}{\partial z_j}\phi_2\right| < \frac{4cR^3}{\delta^3}\left(\left|\frac{\partial\phi_1}{\partial z_1}\right| + \left|\frac{\partial\phi_1}{\partial z_2}\right|\right)|\phi_2|. \tag{21}$$

Consequently, from (19) and (21), we can obtain the coercivity property of the sesquilinear form. Namely, we obtain

$$\begin{aligned}
\sigma(q_1)(\phi,\phi) &> \frac{c}{4R^2}\int_C \sum_{i\le 2}\left|\frac{\partial\phi}{\partial z_i}\right|^2 dz - \frac{4cR^3}{\delta^3}\int_C\sum_{i\le 2}\left|\frac{\partial\phi}{\partial z_i}\right||\phi|\,dz \\
&\ge \frac{c}{8R^2}\int_C\Big(\sum_{i\le 2}\left|\frac{\partial\phi}{\partial z_i}\right|^2 + |\phi|^2\Big)dz \\
&\quad -\frac{c(512R^{10}+\delta^6)}{8\delta^6R^2}\int_C|\phi|^2\,dz.
\end{aligned}$$

Hence there exist constants α and λ such that (12) holds.

To prove the boundedness of $\sigma(q_1)$, we note that

$$|\sigma(q_1)(\phi_1,\phi_2)| \leq$$
$$c\left|\int_C \{\det(\nabla T(q_1))\}^{-2} \sum_{i,j\leq 2} a_{ij}(z,q_1)\frac{\partial\phi_1}{\partial z_j}\frac{\partial\phi_2}{\partial z_i}dz\right|$$
$$+c\left|\int_C \{\det(\nabla T(q_1))\}^{-3} \sum_{j\leq 2} b_j(z,q_1)\frac{\partial\phi_1}{\partial z_j}\phi_2 dz\right|.$$

Using (18) and (C-2), we can estimate the first integral above by

$$c\left|\int_C \{\det(\nabla T(q_1))\}^{-2} \sum_{i,j\leq 2} a_{ij}(z,q_1)\frac{\partial\phi_1}{\partial z_j}\frac{\partial\phi_2}{\partial z_i}dz\right| < \frac{2\sqrt{2}cR^2}{\delta^2}\,|\phi_1|_{H^1(C)}\,|\phi_2|_{H^1(C)}.$$

A similar bound for the second term follows from the use of the estimate in (21) and then (13) follows.

To establish the continuity property of (14), we note that, for any $q_1, \tilde{q}_1 \in Q_1$ and $\phi_1, \phi_2 \in H^1(C)$,

$$|\sigma(q_1)(\phi_1,\phi_2) - \sigma(\tilde{q}_1)(\phi_1,\phi_2)| \leq$$
$$c\left|\int_C \sum_{i,j\leq 2}\left[\{\det(\nabla T(q_1))\}^{-2}a_{ij}(z,q_1) - \{\det(\nabla T(\tilde{q}_1))\}^{-2}a_{ij}(z,\tilde{q}_1)\right]\frac{\partial\phi_1}{\partial z_j}\frac{\partial\phi_2}{\partial z_i}dz\right|$$
$$+c\left|\int_C \sum_{j\leq 2}\left[\{\det(\nabla T(q_1))\}^{-3}b_j(z,q_1) - \{\det(\nabla T(\tilde{q}_1))\}^{-3}b_j(z,\tilde{q}_1)\right]\frac{\partial\phi_1}{\partial z_j}\phi_2 dz\right|.$$

Using (18) and the condition (C-3), we may argue that

$$|a_{ij}(z,q_1) - a_{ij}(z,\tilde{q}_1)| < 4RK_1\,|q_1 - \tilde{q}_1| \qquad \text{for} \quad i,j = 1,2.$$

Similarly, from (20) and (C-3), we have

$$\left|\{\det(\nabla T(q_1))\}^{-2} - \{\det(\nabla T(\tilde{q}_1))\}^{-2}\right| < \frac{2RK_1}{\delta^4}\,|q_1 - \tilde{q}_1|$$

$$\left|\{\det(\nabla T(q_1))\}^{-3} - \{\det(\nabla T(\tilde{q}_1))\}^{-3}\right| < \frac{3R^2K_1}{\delta^6}\,|q_1 - \tilde{q}_1|.$$

Hence we have

$$
\begin{aligned}
&|b_i(z,q_1)-b_i(z,\tilde{q}_1)| \le \\
&\quad |a_{i1}(z,q_1)-a_{i1}(z,\tilde{q}_1)|\left|\frac{\partial}{\partial z_1}\{\det(\nabla T(q_1))\}\right| \\
&\quad + |a_{i1}(z,\tilde{q}_1)|\left|\frac{\partial}{\partial z_1}\{\det(\nabla T(q_1))\}-\frac{\partial}{\partial z_1}\{\det(\nabla T(\tilde{q}_1))\}\right| \\
&\quad + |a_{i2}(z,q_1)-a_{i2}(z,\tilde{q}_1)|\left|\frac{\partial}{\partial z_2}\{\det(\nabla T(q_1))\}\right| \\
&\quad + |a_{i2}(z,\tilde{q}_1)|\left|\frac{\partial}{\partial z_2}\{\det(\nabla T(q_1))\}-\frac{\partial}{\partial z_2}\{\det(\nabla T(\tilde{q}_1))\}\right| \\
&\quad < 12R^2M\,|q_1-\tilde{q}_1|\,.
\end{aligned}
$$

Thus, we obtain that (14) follows from

$$
\begin{aligned}
&|\sigma(q_1)(\phi_1,\phi_2)-\sigma(\tilde{q}_1)(\phi_1,\phi_2)| \\
&\quad < \frac{4cRK_1}{\delta^2}\left(\frac{3R^3}{\delta^4}+\frac{\sqrt{2}R^2}{\delta^2}+\frac{3}{\delta}+\sqrt{2}\right)|q_1-\tilde{q}_1|\,|\phi_1|_{H^1(C)}\,|\phi_2|_{H^1(C)}\,.
\end{aligned}
$$

We introduce a Hilbert space

$$
\mathcal{W}(\mathcal{T})=\left\{\phi\,\middle|\quad \phi\in L^2(\mathcal{T};H^1(C)),\quad \frac{d\phi}{dt}\in L^2(\mathcal{T};(H^1(C))^*)\right\}
$$

endowed with the norm

$$
|\phi|_{\mathcal{W}(\mathcal{T})}=\left\{\int_{t_0}^{t_f}|\phi|^2_{H^1(C)}\,dt+\int_{t_0}^{t_f}\left|\frac{d\phi}{dt}\right|^2_{(H^1(C))^*}dt\right\}^{\frac{1}{2}}
$$

where $(H^1(C))^*$ denotes the dual space of $H^1(C)$. Then we have the following result (see [13, Chapter 3, Theorem 1.2]).

Lemma 1: In addition to the hypotheses (H-0), (H-1) and the conditions (C-1) - (C-3) in Proposition 1, we assume that

(C-4) For each $q\in Q$, we have

$$
\tilde{u}_0(q)\in L^2(C);
$$

(C-5) For each $q_0 \in Q_0$, we have

$$f(q_0) \in L^2(S).$$

Then, for each fixed $q \in Q$, the system (8), (9) possesses a unique solution $\tilde{u}(q)$ in $\mathcal{W}(\mathcal{T})$.

We next formulate a boundary identification problem. In doing so, we must specify a method of data acquisition for the parabolic system (8), (9). Let $\{\xi_p^i\}_{i=1}^m$ be given sensor locations on the surface S. For each observation point $\xi_p^i \in S$, we introduce the observation region $\Sigma_p^i \subset S$ such that

$$\Sigma_p^i = N(\xi_p^i) \cap S \qquad \text{for} \quad i = 1, 2, \cdots, m,$$

where $N(\xi_p^i)$ denotes a neighborhood of the point ξ_p^i. Then the observation mechanism for the system (8), (9) is given by

$$\tilde{y}(t,q) = \mathcal{H}(t)\tilde{u}(t,q) \tag{22}$$

where $\mathcal{H}(t) : H^1(C) \to R^m$ is given by

$$\mathcal{H}_i(t)\phi = \frac{1}{meas(\Sigma_p^i)} \int_{\Sigma_p^i} h_i(t)(\gamma_S \phi) d\xi_S \tag{23}$$

for $i = 1, 2, \cdots, m$. Here the h_i denote the weighting or mollifying functions for the measurement equipment (an infrared camera in the experiments discussed below). We make the following assumption for the observations.

(C-6) For each $i = 1, 2, \cdots, m$, we have $h_i \in L^\infty(\mathcal{T} \times \Sigma_p^i)$.

Then recalling (See [13, Chapter 1, Theorem 3.2]) that the trace map is continuous from $H^1(C)$ to $L^2(S)$, we have for $\tilde{u}(q) \in L^2(\mathcal{T}; H^1(C))$ that

$$\tilde{y}(t,q) = \mathcal{H}(t)\tilde{u}(t,q)$$

is well defined with $\tilde{y}(q) \in L^2(\mathcal{T}; R^m)$. We may then define the fit-to-data criterion function used in our identification problems by

$$J(q) = \frac{1}{2} \int_{t_0}^{t_f} |\tilde{y}(t,q) - y_d(t)|^2 \, dt \tag{24}$$

where $y_d(t)$ denotes the given observed data. Our identification problem may be stated as follows:

(IDP) Find $q^* \in Q$ which minimizes $J(q)$ given by (24) subject to (8), (9).

To insure existence of solutions to (IDP), additional assumptions on the regularity of $\tilde{u}_0$ and f are required. We assume:

(C-7) The mapping $q \to \tilde{u}_0(q)$ is continuous from Q to $L^2(C)$.

(C-8) The mapping $q_0 \to f(q_0)$ is continuous from Q_0 to $L^2(S)$.

Using continuity properties of the trace map γ_S, lower semicontinuity arguments, and the compactness of Q, it is not difficult to prove directly that solutions of (IDP) exist. However, these existence results will also follow directly from the approximation considerations in the next section (See Theorem 2).

III. A COMPUTATIONAL METHOD FOR DOMAIN IDENTIFICATION

In this section, we consider computational techniques for approximate identification problems. The approximation scheme we have employed is based on the use of a finite element Galerkin approach to construct a sequence of finite dimensional approximating identification problems. Let us choose $\bigcup_{N=1}^{\infty}\{\phi_i^N\}_{i=1}^N$ as a set of basis functions in $H^1(C)$. That is, for each $N, \{\phi_i^N\}_{i=1}^N$ are linearly independent and $\bigcup_N span\{\phi_i^N\}_{i=1}^N$ is dense in $H^1(C)$. We choose the approximation subspaces as

$$H^N = span\{\phi_1^N, \phi_2^N, \cdots, \phi_N^N\}.$$

Then, we can define an approximate solution of (8) by

$$\tilde{u}^N(t,q) = \sum_{i \le N} w_i^N(t,q)\phi_i^N$$

where the $w_i^N(t,q)$ are chosen such that, for $j = 1, 2, \cdots, N$,

$$\left\langle \frac{d\tilde{u}^N(t,q)}{dt}, \phi_j^N \right\rangle + \sigma(q_1)(\tilde{u}^N(t,q), \phi_j^N) = L(q)(\phi_j^N)$$

with

$$\left\langle \tilde{u}^N(t_0), \phi_j^N \right\rangle = \left\langle \tilde{u}_0(q), \phi_j^N \right\rangle .$$

Hence, the system (8), (9) can be approximated by solving the system

$$C^N \dot{w}^N(t) + A^N(q_1) w^N(t) = F^N(q), \tag{25}$$

$$C^N w^N(t_0) = \overline{w}_0^N(q) \tag{26}$$

where

$$\begin{aligned}
[C^N]_{ij} &= < \phi_i^N, \phi_j^N > \quad \text{for } i,j = 1,2,\cdots,N \\
[A^N(q_1)]_{ij} &= \sigma(q_1)(\phi_j^N, \phi_i^N) \quad \text{for } i,j = 1,2,\cdots,N \\
[F^N(q)]_i &= L(q)(\phi_i^N) \quad \text{for } i = 1,2,\cdots,N \\
[w^N(t)]_i &= w_i^N(t) \quad \text{for } i = 1,2,\cdots,N \\
[\overline{w}_0^N]_i &= < \tilde{u}_0(q), \phi_i^N > \quad \text{for } i = 1,2,\cdots,N.
\end{aligned}$$

The corresponding output becomes

$$\tilde{y}^N(t,q) = \mathcal{H}^N(t) w^N(t,q)$$

where $\mathcal{H}^N(q_1)$ is the $m \times N$-matrix given by

$$\left[\mathcal{H}^N(t)\right]_{ij} = \mathcal{H}_i(t)\phi_j^N \qquad \text{for} \quad i = 1,2,\cdots,m; j = 1,2,\cdots,N.$$

Then we seek to solve the approximating identification problem given by:

(AIDP)^N Find $\hat{q}^N \in Q$ which minimizes

$$J^N(q) = \frac{1}{2}\int_{t_0}^{t_f} \left|\tilde{y}^N(t,q) - y_d(t)\right|^2 dt \tag{27}$$

subject to the approximating system (25), (26).

Since it is readily seen that the approximate solution $\tilde{u}^N(q)$ (and hence the maps $\tilde{y}^N(t,q)$) depend continuously on q, we have that solutions to these approximate problems exist for

each N. Our convergence results for the approximate parameter estimates are summarized in the following theorem.

Theorem 2: *Suppose that hypotheses (H-0), (H-1) and (C-1)-(C-8) hold and let* $\hat{q}^N$ *be a solution of the problem* $(\mathrm{AIDP})^N$. *Then the sequence* $\{\hat{q}^N\}$ *admits a convergent subsequence* $\{\hat{q}^{N_k}\}$ *with* $\hat{q}^{N_k} \to q^*$ *as* $N_k \to \infty$. *Moreover,* q^* *is a solution of the problem (IDP).*

Proof: Since $\hat{q}^N$ is a solution of the problem $(AIDP)^N$, it is clear that

$$J^N(\hat{q}^N) \leq J^N(q) \qquad \text{for all } q \in Q.$$

Thus, if we can argue that for any $q^M \to q$ in Q,

$$y^N(q^M) \to y(q) \qquad \text{in} \quad L^2(\mathcal{T}; R^m) \quad \text{as } N, M \to \infty,$$

then, we can obtain the desired inequality

$$J(q^*) \leq J(q) \qquad \text{for all } q \in Q$$

by taking limits in (27). To show this, it suffices to argue that $\tilde{u}^N(q^N) \longrightarrow \tilde{u}(q^*)$ in $L^2(\mathcal{T}; H^1(C))$ as $N \to \infty$ for arbitrary sequences $\{q^N\}$ with $q^N \to q^*$ as $N \to \infty$. This follows since the output mapping $\mathcal{H}$ is continuous from $L^2(\mathcal{T}; H^1(C))$ to $L^2(\mathcal{T}; R^m)$ (recall that γ_S is continuous from $H^1(C)$ to $L^2(S)$ and $h_i \in L^\infty(\mathcal{T} \times \Sigma_p^i)$).

To argue this convergence of $\tilde{u}^N(q^N)$ to $\tilde{u}(q^*)$ in $L^2(\mathcal{T}; H^1(C))$, one can use the theory developed in [2]. Since Theorem 1 above guarantees conditions (A),(B) and (C) of [2], and the density of $\cup_N H^N$ in $H^1(C)$ guarantees that (C1) of [2] holds, we only need observe that (8), (9) can be written in the form (in $H = L^2(C)$)

$$\dot{u}(t) = A(q)u(t) + F(q) \tag{28}$$

as required in [2]. The only question to address is that of whether our L as given in (11) gives rise to an $F(q)$ with values in $L^2(C)$ (in the notation of [2], we have $H = L^2(C), V = H^1(C)$). From (11) and the continuity of $\gamma_S : H^1(C) \to L^2(S)$, we see that $\phi \to L(q)(\phi)$ is in V^*.

Since V is dense in $H = L^2(C)$, we can extend (by continuity) in the usual manner so that the weak system (8) can be equivalently written in the form (28). The desired convergence results then follow from Theorem 2.3 of [2] along with the representations (2.2) and (2.6) of [2].

IV. PRACTICAL IMPLEMENTATION

In order to implement the identification scheme proposed in Section 3, we need to construct the mapping operator $T(q_1)$. In this section, we treat the special case of identification of a boundary shape $\Gamma(q_1)$ characterized by a simple function. We consider the bounded domain $G(q_1)$ in R^2 as follows:

$$G(q_1) = \left\{ x \in R^2 \mid 0 < x_1 < 1,\ 0 < x_2 < r(x_1, q_1) \right\}$$

where $x_1 \rightarrow r(x_1, q_1)$ is some parametrized real function which is assumed to characterize the unknown part (the possible corrosive region) of the boundary $\Gamma(q_1)$ as depicted in Fig. 3. We assume that the boundary of $G(q_1)$ consists of

$$\partial G(q_1) = S \bigcup \Gamma(q_1)$$

$$\begin{aligned} \Gamma(q_1) = \{x | 0 \le x_1 \le 1, x_2 = r(x_1, q_1) \text{ with } \quad r(0, q_1) = r(1, q_1) = l\} \\ \bigcup \{x | x_1 = 0, 0 < x_2 < l\} \bigcup \{x | x_1 = 1, 0 < x_2 < l\} \end{aligned}$$

$$S = \{x | 0 \le x_1 \le 1, x_2 = 0\}.$$

We use the reference domain $C = (0,1) \times (0,l)$ and we introduce the mapping from C into $G(q_1)$,

$$x = T(q_1)(z)$$

$$\begin{cases} x_1 = \psi_1(z, q_1) = z_1 \\ x_2 = \psi_2(z, q_1) = \frac{r(z_1, q_1) z_2}{l} \end{cases} . \tag{29}$$

Then it is easy to verify that this mapping $T(q_1)$ satisfies hypothesis (H-1). Noting that

$$\nabla T(q_1) = \begin{bmatrix} 1 & \frac{r'(z_1, q_1) z_2}{l} \\ 0 & \frac{r(z_1, q_1)}{l} \end{bmatrix},$$

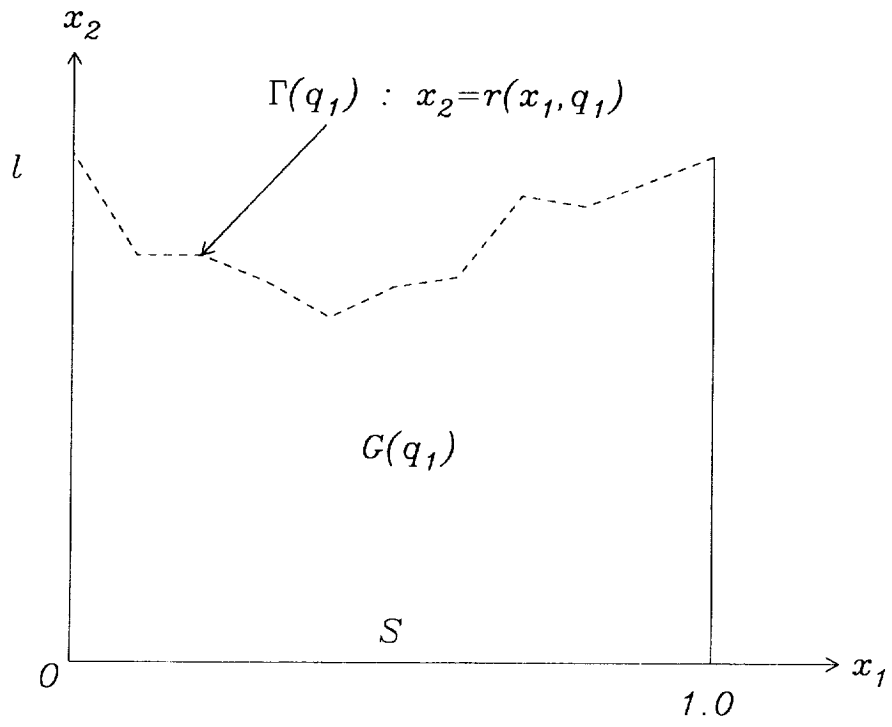

Figure 3. The unknown spatial domain

we find that the coefficients in the sesquilinear form (10) are given by

$$(\nabla T(q_1))^{-t}(\nabla T(q_1))^{-1} = \begin{bmatrix} 1 & -\frac{r'(z_1,q_1)z_2}{r(z_1,q_1)} \\ -\frac{r'(z_1,q_1)z_2}{r(z_1,q_1)} & \frac{1}{(r(z_1,q_1))^2}\{(r'(z_1,q_1))^2 z_2^2 + l^2\} \end{bmatrix}$$

$$-\{\det(\nabla T(q_1))\}^{-1}(\nabla T(q_1))^{-t}(\nabla T(q_1))^{-1}\{\nabla \det(\nabla T(q_1))\} = \begin{bmatrix} -\frac{r'(z_1,q_1)}{r(z_1,q_1)} \\ \frac{(r'(z_1,q_1))^2 z_2}{(r(z_1,q_1))^2} \end{bmatrix}.$$

Furthermore, it follows that

$$\det(\nabla T(q_1)) = \frac{r(z_1,q_1)}{l}.$$

Hence, the sesquilinear form $\sigma(q_1)$ in this case is explicitly given by

$$\begin{aligned} \sigma(q_1)(\phi,\psi) \;=\; & \int_0^l \int_0^1 c \left[\frac{\partial\phi}{\partial z_1}\frac{\partial\psi}{\partial z_1} - \frac{r'(z_1,q_1)z_2}{r(z_1,q_1)} \left(\frac{\partial\phi}{\partial z_2}\frac{\partial\psi}{\partial z_1} + \frac{\partial\phi}{\partial z_1}\frac{\partial\psi}{\partial z_2} \right) \right. \\ & + \frac{1}{(r(z_1,q_1))^2}\left\{(r'(z_1,q_1))^2 z_2^2 + l^2\right\}\frac{\partial\phi}{\partial z_2}\frac{\partial\psi}{\partial z_2} - \frac{r'(z_1,q_1)}{r(z_1,q_1)}\frac{\partial\phi}{\partial z_1}\psi \\ & \left. + \frac{(r'(z_1,q_1))^2 z_2}{(r(z_1,q_1))^2}\frac{\partial\phi}{\partial z_2}\psi \right] dz_1 dz_2. \end{aligned} \tag{30}$$

The linear form $L(q)$ of (11) in this case has the representation

$$L(q)(\phi) = \int_0^1 \frac{lf(z_1, q_0)}{r(z_1, q_1)} \phi(z_1, 0) dz_1. \tag{31}$$

Lemma 2: Suppose that

(C-9) For each $q_1 \in Q_1$, $r(q_1)$ belongs to $W_\infty^1(0,1)$;

(C-10) There exists a constant ν_1 such that for each $q_1 \in Q_1$,

$$r(z_1, q_1) \geq \nu_1 > 0;$$

(C-11) There exists a constant ν_2 such that for each $q_1, \tilde{q}_1 \in Q_1$,

$$|r(z_1, q_1) - r(z_1, \tilde{q}_1)|_{W_\infty^1(0,1)} \leq \nu_2 |q_1 - \tilde{q}_1|.$$

Then the mapping $T(q_1)$ given by (29) satisfies the conditions (C-1) to (C-3) in Theorem 1.

From Lemma 2, under the conditions (C-9) to (C-11), we can apply the domain identification techniques as outlined in the previous sections to the problem posed in this section. In the sequel, we consider linear spline approximations of parameterized functions for r and f. For $k = 0, 1$, let $L(\triangle^{M_k})$ be the set of piecewise linear splines (see [6] for details) with the knot sequence $\triangle^{M_k} = \{i/M_k\}_{i=0}^{M_k}$ and basis elements $\{B_i^{M_k}\}$. Then we approximate the unknown input function and the unknown corrosion shape function by

$$\tilde{f}(\zeta, q_0) = \sum_{i=0}^{\bar{M}_0 - 1} \eta_i^{M_0} B_i^{M_0}(\zeta) + \sum_{i=\bar{M}_0}^{\bar{M}_0 + n_0 - 1} q_0^{i - \bar{M}_0} B_i^{M_0}(\zeta) + \sum_{i=\bar{M}_0 + n_0}^{M_0} \eta_i^{M_0} B_i^{M_0}(\zeta) \tag{32}$$

and

$$\tilde{r}(\zeta, q_1) = \sum_{i=0}^{\bar{M}_1 - 1} \theta_i^{M_1} B_i^{M_1}(\zeta) + \sum_{i=\bar{M}_1}^{\bar{M}_1 + n_1 - 1} q_1^{i - \bar{M}_1} B_i^{M_1}(\zeta) + \sum_{i=\bar{M}_1 + n_1}^{M_1} \theta_i^{M_1} B_i^{M_1}(\zeta), \tag{33}$$

respectively. Here we assume that the η_i and θ_i are fixed and the q_i are to be estimated. In order to ensure the hypotheses of Lemma 2, we impose constraints on $Q \equiv Q_0 \times Q_1$ with

$$Q_k = \left\{ q_k \in R^{n_k} \;\middle|\; \bar{q}_k^L \leq q_k \leq \bar{q}_k^U \right\}, \quad k = 0, 1, \tag{34}$$

where $\bar{q}_k^L$ and $\bar{q}_k^U$ are given lower and upper bounds, respectively. The bounds $\bar{q}_1^L$ and $\bar{q}_1^U$ are determined by ν_1, ν_2 and upper bounds of the corrosion function r and its derivative.

In the reminder of this section, we discuss computer implementation of numerical schemes for the problem $(AIDP)^N$. For the results reported in this paper, we solved the numerical optimization problems using a trust region algorithm. Our trust region scheme can be briefly stated as follows: Let $\{q_k = (q_{0k}, q_{1k})\}_{k=1,2,\ldots}$ be a sequence generated by this algorithm. At the current point q_k, we build a "model" of the cost functional (we usually choose a quadratic model). Then we define a region around q_k where we believe this model to be an adequate approximation of the functional. Using this model, we seek a feasible direction so as to guarantee a sufficient decrease in the model of cost. Once we obtain the feasible direction, the exact cost functional is evaluated at the new point. If its value has decreased sufficiently, this new point is accepted and updated as the next iterate, and a new trust region is selected for the next iteration. Otherwise the new point is rejected and the current trust region is reduced. The advantage of this algorithm is its global convergence properties;namely, this algorithm makes it possible to obtain convergence to a critical point (optimal solution), even from starting points (initial guesses) that are far away from the optimal solution. For detailed discussions, we refer to [7] and [14].

For the implementation of the trust region algorithm, we used a Fortran software package "OPT" created by Dr. Richard Carter of ICASE (see [7] for details). Test computations were carried out on the Cray-2S at NASA Langley Research Center.

V. NUMERICAL EXPERIMENTS

Throughout both our computational and laboratory experiments, we considered corrosion shape identification for steel samples with corrosion like damage (of varying size and corrosion depth) as depicted in Fig. 4. Since the sample material was steel, the thermal diffusivity coefficient c in (1) was taken as $c = 3.18611 \times 10^{-2}$ ($(\text{inch})^2/\text{sec}$). The first part of this section is devoted to a summary of computational experiments for the purpose of

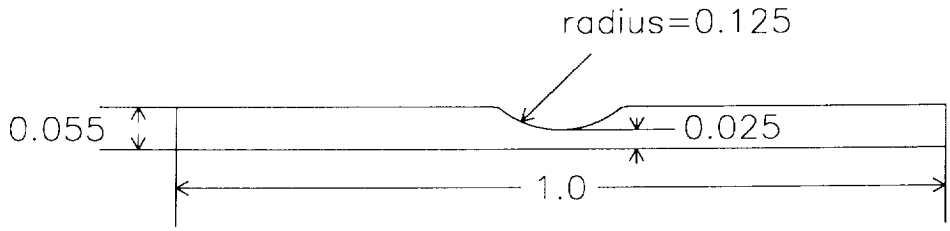

Figure 4. Sample material with corrosion used in one of the experiments

better understanding our computational method. This is followed by a discussion in which the feasibility and validity of our algorithm using laboratory data is demonstrated.

V.1. Computational Experiments with Simulated Data

In our numerical experiments, we used a test example constructed as follows: We chose a 'true' parameter vector $q^o = (q_0^o, q_1^o) \in Q$, generated the corresponding solution numerically, added random noise, and then used this as "data" for our inverse algorithm. In this procedure, the dimensions of the unknown parameter vectors were taken as $dim(q_0) = n_0 = 5$, $dim(q_1) = n_1 = 5$. The corresponding numbers of knot sequences in (32) and (33) were chosen as $M_0 = 4, \bar{M}_0 = 0$ (i. e., all the coefficients for $\tilde{f}$ were to be estimated), $M_1 = 32, \bar{M}_1 = 14$, respectively. The value of the true parameters were chosen as

$$q_0^o = [1.8,\ 1.8,\ 1.8,\ 1.8,\ 1.8],$$

$$q_1^o = [0.0417468,\ 0.0289693,\ 0.0250000,\ 0.0289693,\ 0.0417468].$$

Figure 5 depicts the true curve approximated by piecewise linear splines. In order to guarantee the conditions (C-9) - (C-11), the constrained sets Q_0 and Q_1 defining Q in (34) were taken as

$$Q_0 = \left\{ q_0 \in R^5 \,\middle|\, 0.15 \le q_0^i \le 0.25, \quad i = 1,2,3,4,5 \right\}$$

and

$$Q_1 = \left\{ q_1 \in R^5 \,\middle|\, 0.01 \le q_1^i \le 0.055, \quad i = 1,2,3,4,5 \right\},$$

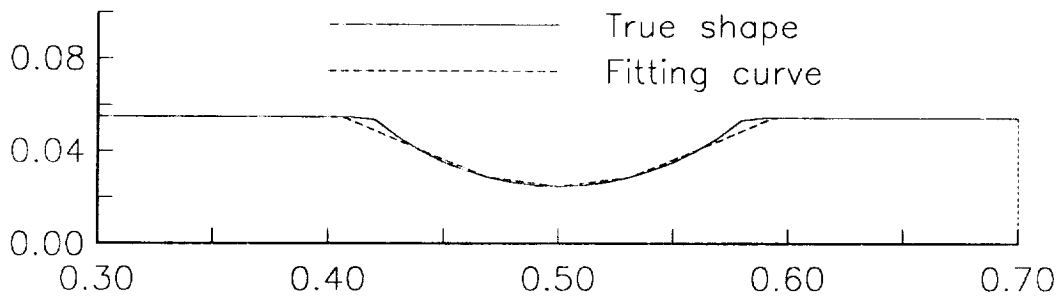

Figure 5. The corrosion shape and the approximating linear spline curve

respectively. The initial state function was preassigned as

$$\bar{u}_0(q, x) = 0 \qquad \text{in} \quad G(q_1).$$

Then we have

$$\begin{aligned} \tilde{u}_0(q) &= \bar{u}_0(x) \circ T(q_1) \\ &= 0 \qquad \text{in} \quad C. \end{aligned}$$

To discretize the system model by a (bilinear spline) finite element method, the reference domain C is divided into a finite number of elements $\{e_k\}_{k=1}^{K}$ $(K \leq N)$ and a number N of nodes defined by $\{z_i = (z_1^i, z_2^i)\}_{i=1}^{N}$ are selected in C. Each element is preassigned as an axiparallel rectangle with nodes at the vertices as shown in Fig. 6. The number of finite elements and nodes in the numerical experiments reported on here were set as

Figure 6. The decomposition of finite elements in C

$K = 128\ (= 32 \times 4)$ and $N = 165\ (= 33 \times 5)$, respectively. The restriction of ϕ_i^N to any element e_k is given by a bilinear polynomial of the form,

$$\phi_i^N(z) = (a_{i,k}^{(10)} + a_{i,k}^{(11)} z_1)(a_{i,k}^{(20)} + a_{i,k}^{(21)} z_2)$$

$$\text{for } z = (z_1, z_2) \in e_k \qquad k = 1, 2, \cdots, K \qquad \text{and} \qquad i = 1, 2, \cdots, N.$$

The coefficients $\{a_{i,k}^{(lj)}\}$ can be chosen such that each polynomial form satisfies the properties of a piecewise bilinear basis function (see e.g., [1, Chapter 5]). Integration in the element matrices $C^N, A^N(q_1)$ and the element vector $F^N(q)$ can be computed numerically by a Gauss-Legendre formula. Thus, the state model (8), (9) can be solved numerically by an implicit scheme with respect to discrete time $t = t_0 + ih$ $(i = 0, 1, \cdots, m_t)$ where $h = (t_f - t_0)/m_t$. The initial and final time, and number of time divisions were taken as $t_0 = 0., t_f = 10.$ and $m_t = 80$ in our computations. To obtain the output, the weighting functions in the measurement operator were given by

$$h_i(t) = \begin{cases} 0. & \text{for} \quad i = 1, 2, \cdots, m \text{ and } 0. \leq t \leq 1. \\ 1. & \text{for} \quad i = 1, 2, \cdots, m \text{ and } 1. \leq t \leq 4. \end{cases}$$

The number of observation points was set as $m = 25$ and sensors are located at

$$\xi_p^i = (z_1, z_2) = \left(\frac{i-1}{32} + 0.125,\ 0\right) \quad \text{for} \quad i = 1, 2, \cdots, 25.$$

For these test example computations, simulated data $\{y_d(t)\}$ were generated by first solving the finite element model (25), (26) with the same number (as used in the model solution) of finite elements and nodes. Random noise at various levels from 0% to 50% was then added to the numerical solution, thereby producing simulated noisy "data" for the algorithm.

The evaluations of the cost functional J^N, its gradient $\nabla_q J^N$ and its Hessian matrix are the computationally expensive parts of our algorithm since these involve integration of the states $w^N(t, q)$ with respect to time t over $\mathcal{T}$. This can be accomplished by using the trapezoidal rule in the Newton-Cotes formula. The gradient and the corresponding

Hessian are computed using a forward difference scheme and the BFGS secant update with safeguarding Hessian approximation (see [7]). In each experiment, the optimization routine was implemented using rectangular trust regions.

Table 1 reports the estimated parameter results for the data without noise and with 5, 10, 15 and 20% relative noise. Figures 7 - 11 represent the value of cost function, and the estimated parameter functions $\tilde{f}(z_1, \hat{q}_0)$ and $\tilde{r}(z_1, \hat{q}_1)$ which correspond to the estimated boundary input and boundary (corrosion) shape, respectively. These and other test computations (see also [4]) suggest that the methods perform well with reasonable levels of noise (20% or less). Tests with higher levels of noise (e. g. 50%) produced results indicating less than satisfactory recovery of reasonable values for the parameters.

Table 1. True value and estimated values of q

	True Value	Noise Free $iter = 61$	5% Noise $iter = 18$	10% Noise $iter = 17$	15% Noise $iter = 15$	20% Noise iter=9
q_0^1	0.1800	0.1800	0.1813	0.1820	0.1770	0.1857
q_0^2	0.1800	0.1800	0.1787	0.1778	0.1809	0.1738
q_0^3	0.1800	0.1799	0.1832	0.1847	0.1859	0.2038
q_0^4	0.1800	0.1800	0.1783	0.1777	0.1797	0.1721
q_0^5	0.1800	0.1800	0.1823	0.1826	0.1799	0.1879
q_1^1	0.04175	0.04165	0.04403	0.04479	0.04444	0.04156
q_1^2	0.02897	0.02896	0.02814	0.02885	0.03195	0.03869
q_1^3	0.02500	0.02509	0.02571	0.02486	0.02755	0.03813
q_1^4	0.02897	0.02894	0.02749	0.02698	0.02730	0.03928
q_1^5	0.04175	0.04166	0.04524	0.04591	0.04668	0.04357
$J(q)$		2.473×10^{-8}	3.626×10^{-2}	1.490×10^{-1}	3.351×10^{-1}	5.899×10^{-1}

(iter = No. of iteration)

V.2. Computational Results Using Experimental Data

In this subsection, we report some of the results of using our estimation procedures with experimental data. A schematic of the experimental system is illustrated in Fig. 12. All

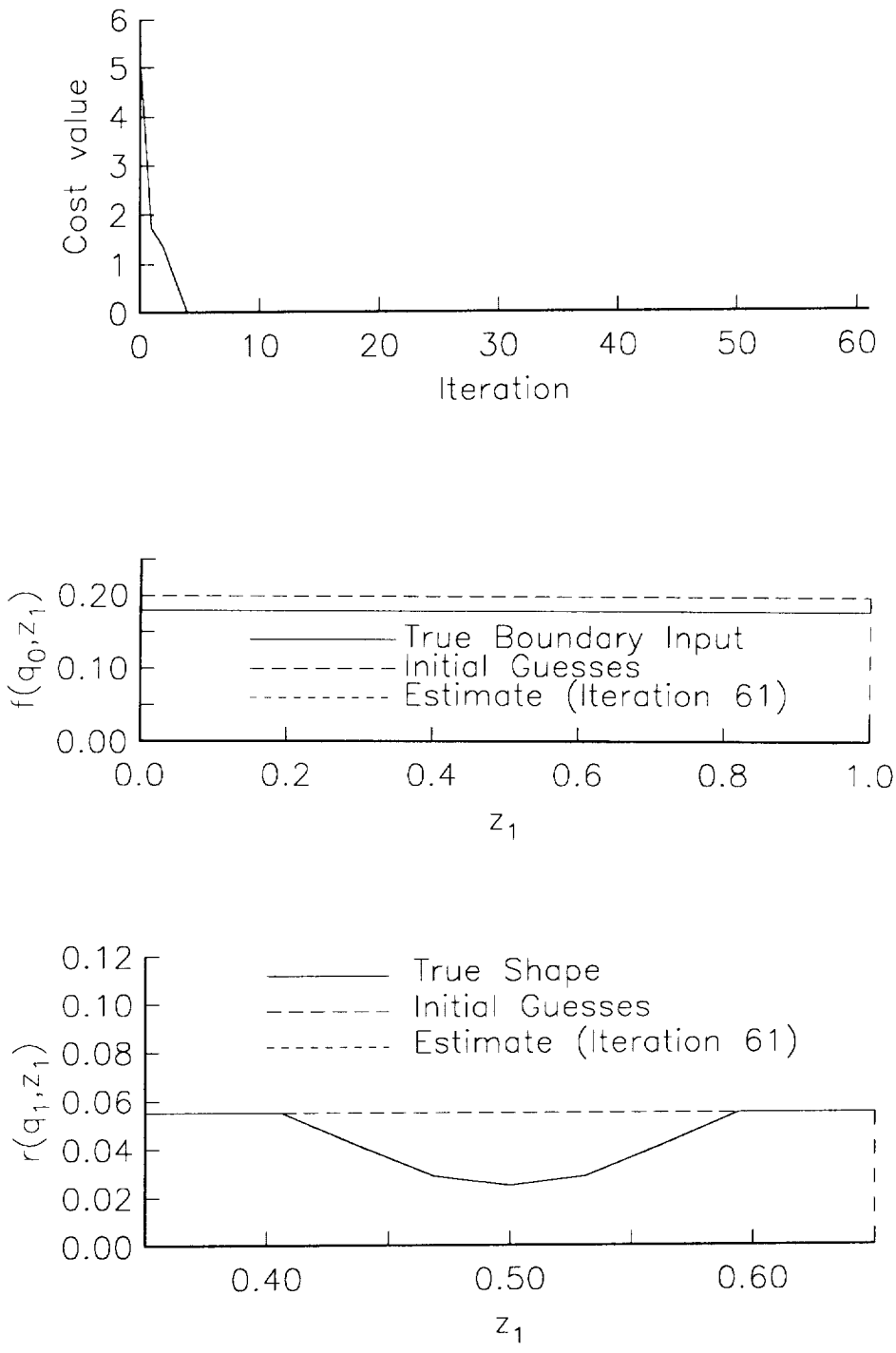

Figure 7. True function and estimated function (Noise Free)

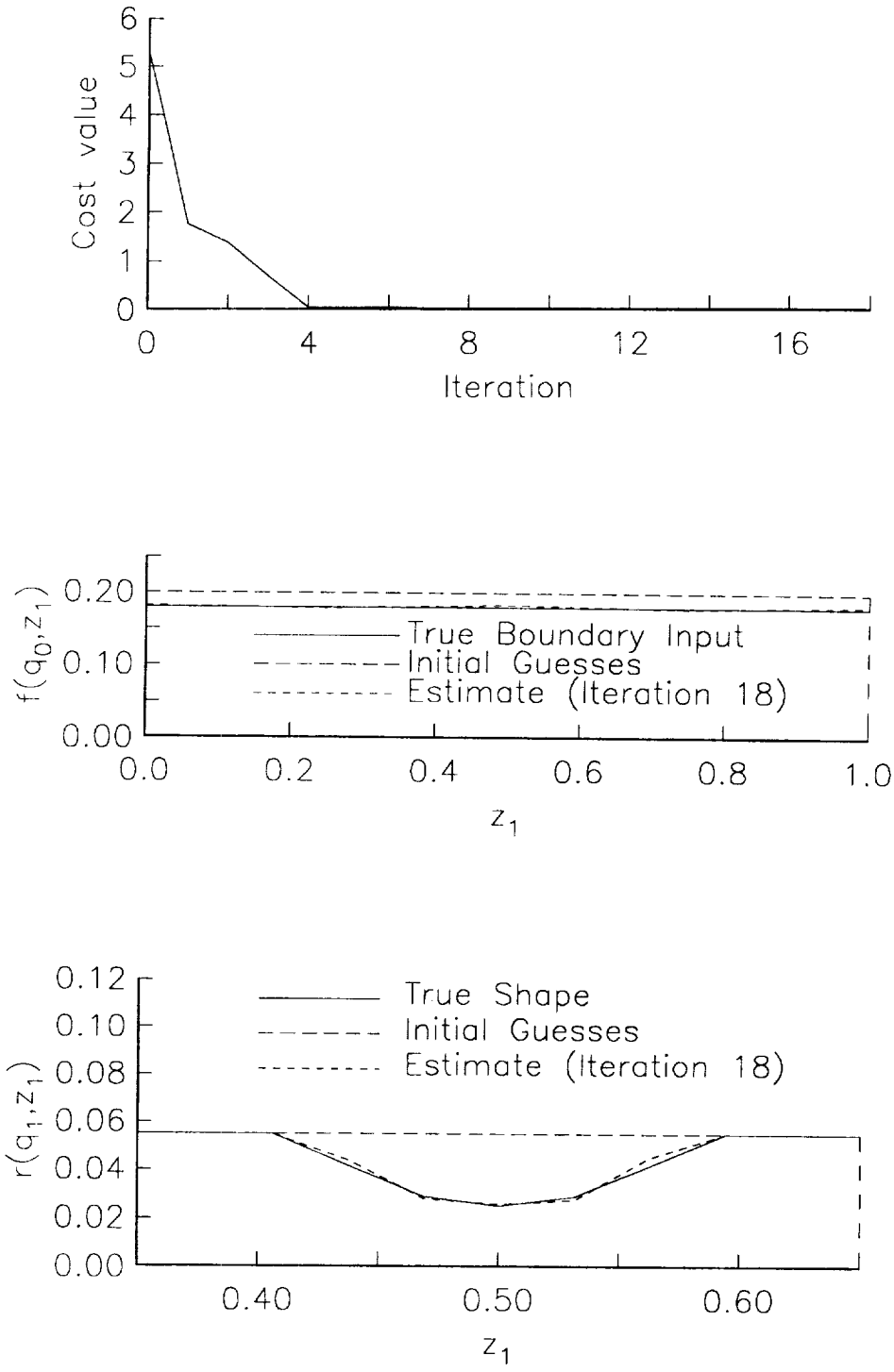

Figure 8. True function and estimated function (5% Noise)

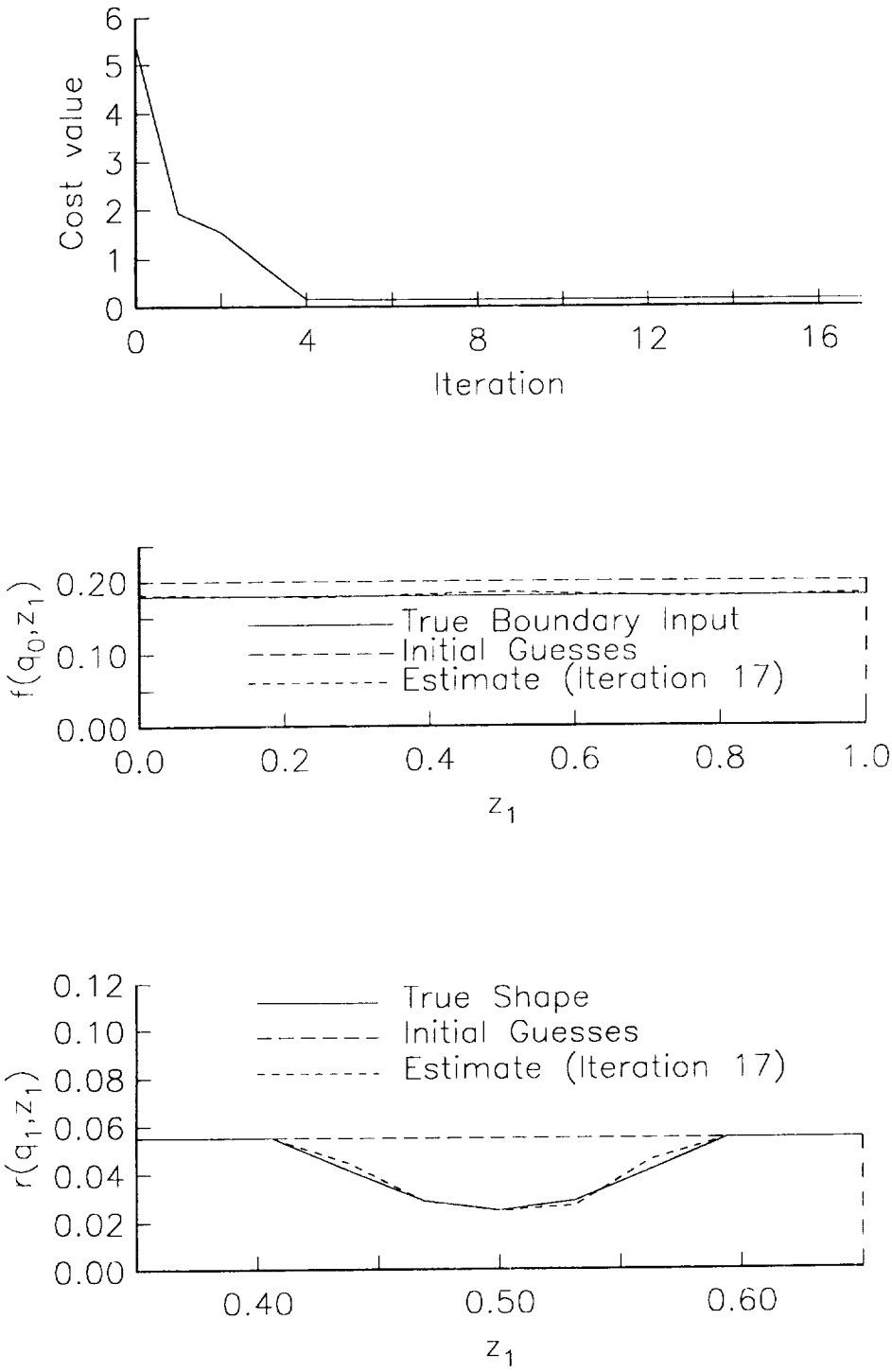

Figure 9. True function and estimated function (10% Noise)

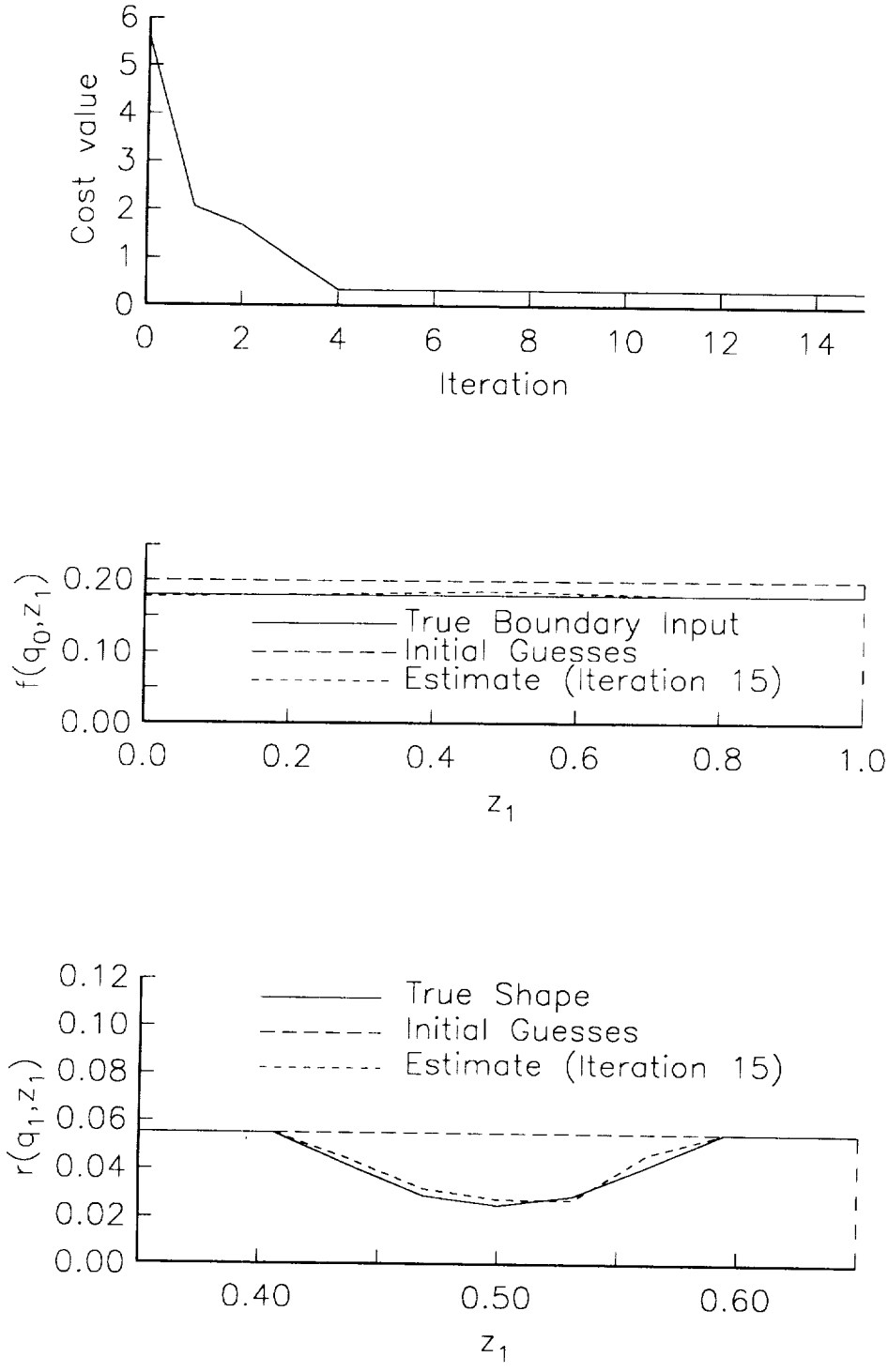

Figure 10. True function and estimated function (15% Noise)

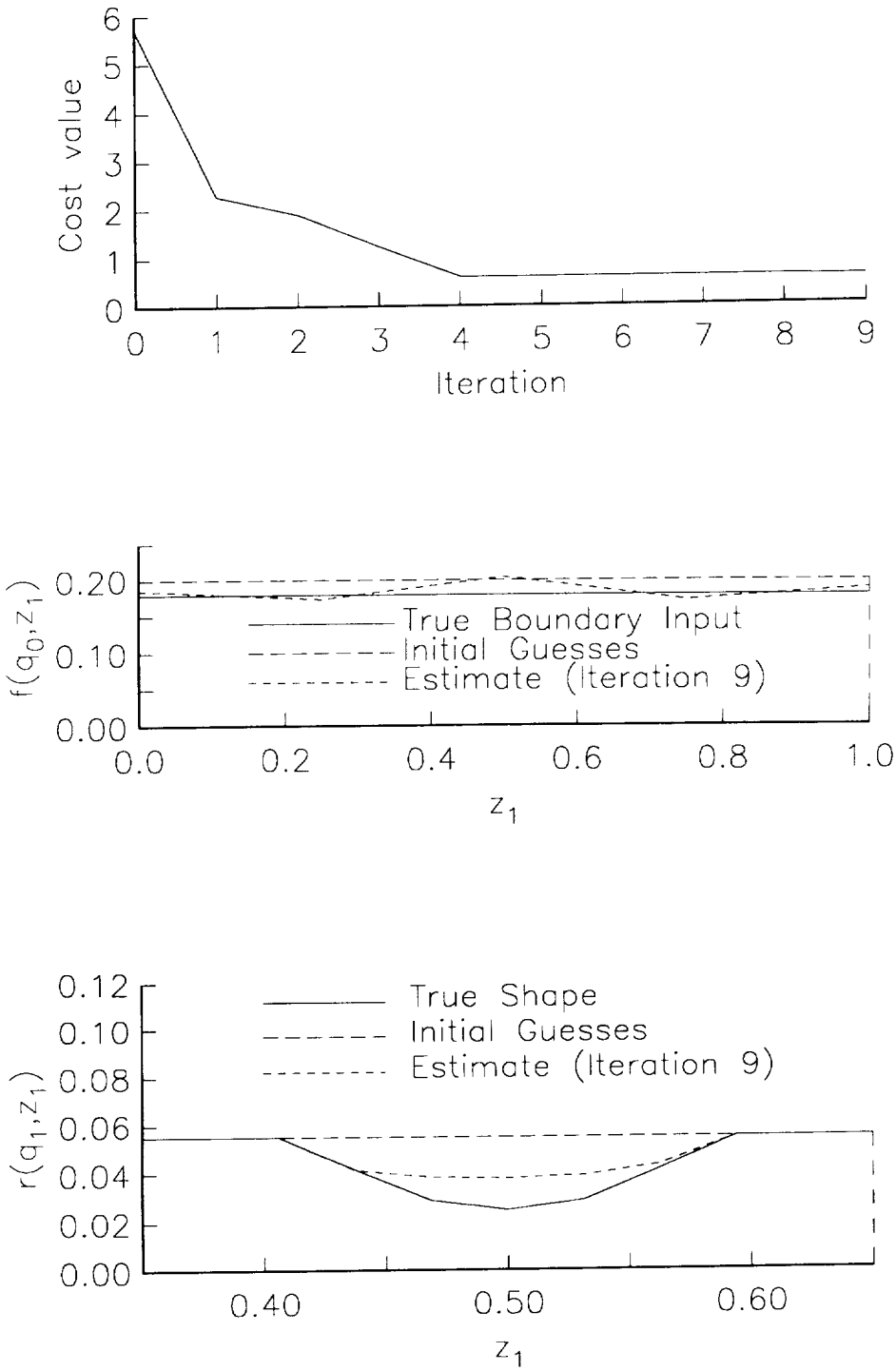

Figure 11. True function and estimated function (20% Noise)

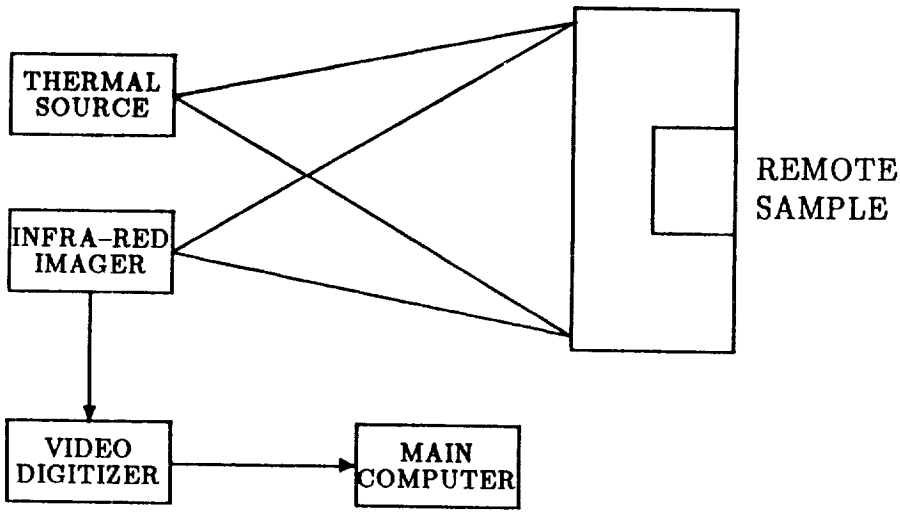

Figure 12. Block diagram of experimental setup

experiments were carried out in the laboratories of the Instrument Reseach Division, Nondestructive Measurement Science Branch, NASA Langley Research Center. The experimental data consisted of surface temperature distributions for a four second period after a thermal source (heat lamps) was provided to a sample. In a series of experiments, two types of material samples were used : one type of sample fabricated to simulate corrosion similar to that shown in Fig. 4 and another type of sample fabricated to simulate no corrosion (an unflawed rectangular sample 0.055 inch by one inch). The measured experimental data are graphed in Fig. 13.

As readily seen in Fig. 13, the unknown boundary flux f is a time-varying function, especially in a neighborhood of the initial time (this is mainly due to the measurement apparutus for the heat source), whereas, in our algorithm, the boundary input is assumed to be a time-invariant function. To handle this discrepancy, noting that the time evolution of the experimental data is linearly increasing after an appropriate time period, we set the initial time as $t_0 = 1.875$ sec. Figure 14 depicts the initial time t_0 and the time evolution of the experimental data (for the sample with corrosion) at the midpoint $x = 0.5$.

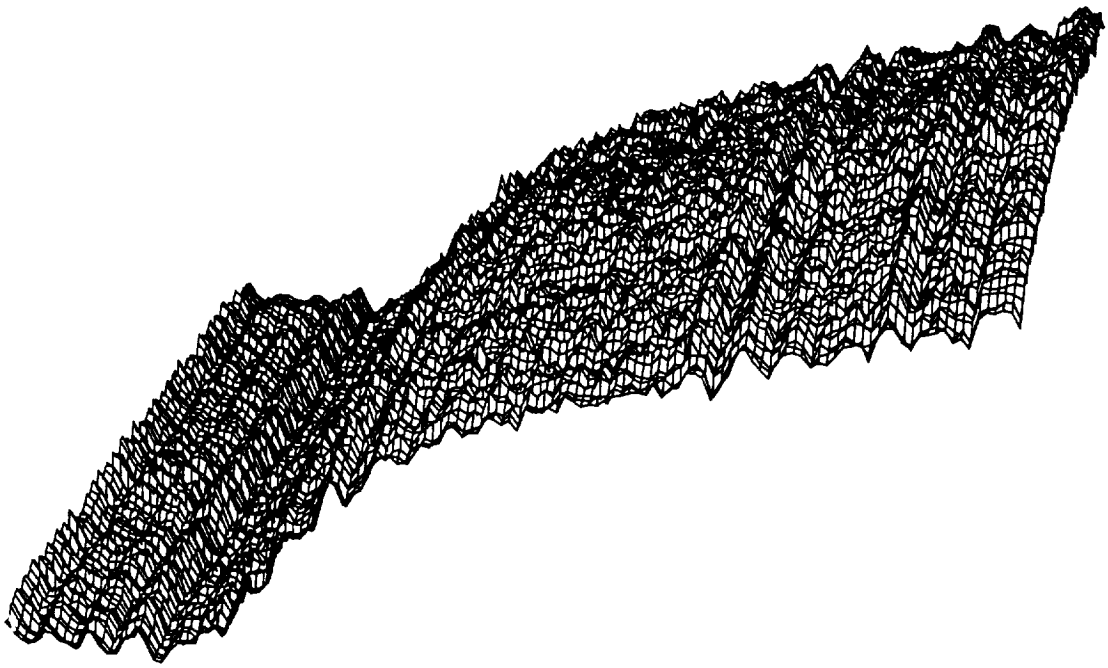

(a) with corrosion

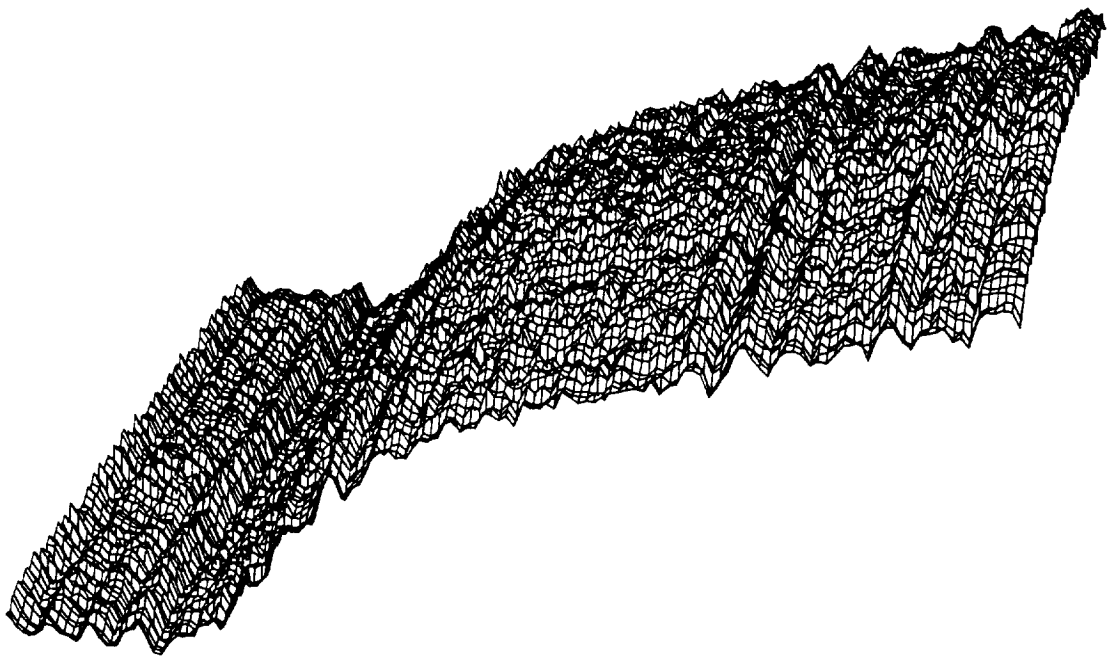

(b) without corrosion

Figure 13. Experimental data (surface temperature)

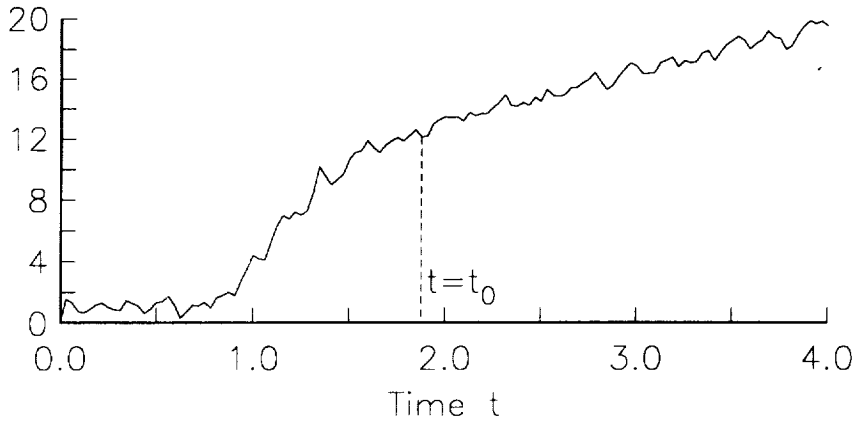

Figure 14. The time evolution of data at $x = 0.5$
(sample with corrosion)

An important feature of the experimental data as depicted in Fig. 15 is that the magnitude of noise is rather high. As demonstrated in the computational experiments of the previous section, this could pose difficulties for our estimation procedures. One possible method for alleviating this dificculty is to use a data smoothing technique. To this end, we used ICSSCU (the IMSL version) which implements a cubic spline data smoothing. Figure 15 compares the smoothed data and the original experimental data at time $t = t_0$ ($= 1.875$).

Another important question which arises in using our algorithm is that of how to preassign the initial data $\overline{u}_0(q)$. We only know the surface data $\gamma_S \overline{u}_0 (= \gamma_S \tilde{u}_0)$ from the boundary surface measurement at time $t = t_0$. One possible solution is to approximate the initial state by the steady state solution of

$$\Delta \overline{u} = 0 \quad \text{in } G(q_1)$$

with the boundary conditions

$$\begin{aligned} \frac{\partial \overline{u}}{\partial n} &= 0 \qquad \text{on } \Gamma(q_1) \\ \overline{u} &= \mathcal{H}^{-1}(t_0) z_d(t_0) \quad \text{on } S, \end{aligned}$$

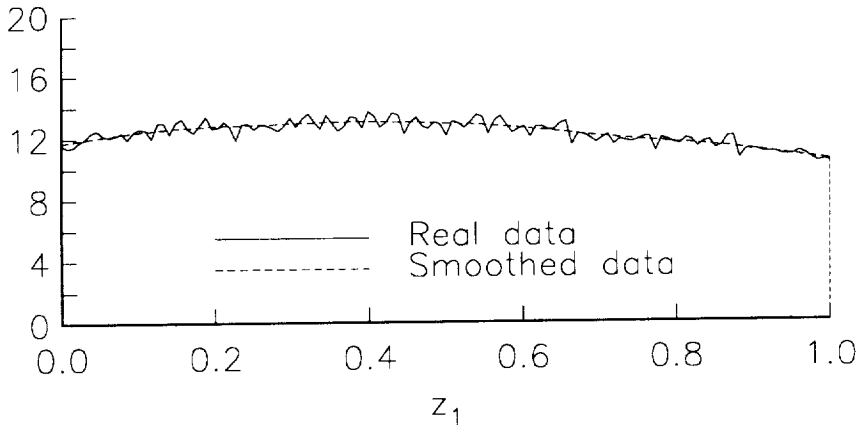

Figure 15. The smoothed data vs. experimental data at time $t = t_0$
(sample with corrosion)

where $z_d(t_0)$ is the observed surface data. We used a finite element method to solve this steady state problem for $\overline{u}(q_1)$ and then set $\tilde{u}_0(q) = \overline{u}(q_1)$.

Inverse problems such as we have considered here may exhibit a lack of continuous dependence of the estimated parameters on the data. This often leads to serious dificulties in computational efforts. It is helpful to use a regularization technique. To this end, for the computer implementation of our algorithm using experimental data, we added a regularization term to the cost function, i. e.,

$$\tilde{J}^N(q) = J^N(q) + \eta \left| \frac{dr}{dz_1}(q_1) \right|^2_{L^2(0,1)}$$

(see e. g. [11], [15]). The results of our estimation procedures for one set of experiments (the sample with corrosion had dimensions as shown in Fig. 4) are given in Table 2 , Fig. 16 and Fig. 17. Similar results for a second set of experiments for different material samples are depicted in Figures 18 and 19 (in this case, a sample with actual dimensions $0.09375 \times 1.$ inch and corrosion radius 0.25 inch was used). Note that in this case our procedures were able to locate a "corrosion" that was not centered in the sample.

Table 2. True value and estimated values of q_0

	With corrosion		Without corrosion	
η	0.	10.	0.	10.
q_0^1	0.2244	0.2244	0.1387	0.1351
q_0^2	0.2892	0.2939	0.3430	0.3462
q_0^3	0.2267	0.2316	0.2451	0.2521
q_0^4	0.2551	0.2554	0.2719	0.2683
q_0^5	0.1958	0.1952	0.3623	0.3653
q_1^1	0.02718	0.04388	0.04466	0.05500
q_1^2	0.03422	0.03662	0.05500	0.05500
q_1^3	0.04128	0.03544	0.05500	0.05500
q_1^4	0.05135	0.03778	0.05500	0.05500
q_1^5	0.03142	0.04404	0.05500	0.05500
$J(q)$	2.215 $\times 10^{-1}$	2.252 $\times 10^{-1}$	3.222 $\times 10^{-1}$	3.222 $\times 10^{-1}$

VI. CONCLUDING REMARKS

In the last section we summarized some of our findings using the methods in this paper with laboratory data. To date, we have used 7 different samples of material (all of steel); at least 17 different experiments were carried out and for each of these experiments we used our estimation packages with the resulting data. The several results reported in detail above are representative of our findings. In all cases, the algorithm performed as well as or better than it did in the examples given above. We believe this provides rather conclusive evidence that (i) structual flaws of this nature can be successfully detected using thermal methods, and (ii) the mathematical and computational ideas presented in this paper can be effectively used in determining the existence, location, and nature of such material flaws. We are currently pursuing both experimental and computational investigations to further refine our methods as well as to test other types of materials (aluminium, etc) and flaws (e. g. delaminations) with regard to ease and accuracy in detection and characterization of flaws using thermal based methods.

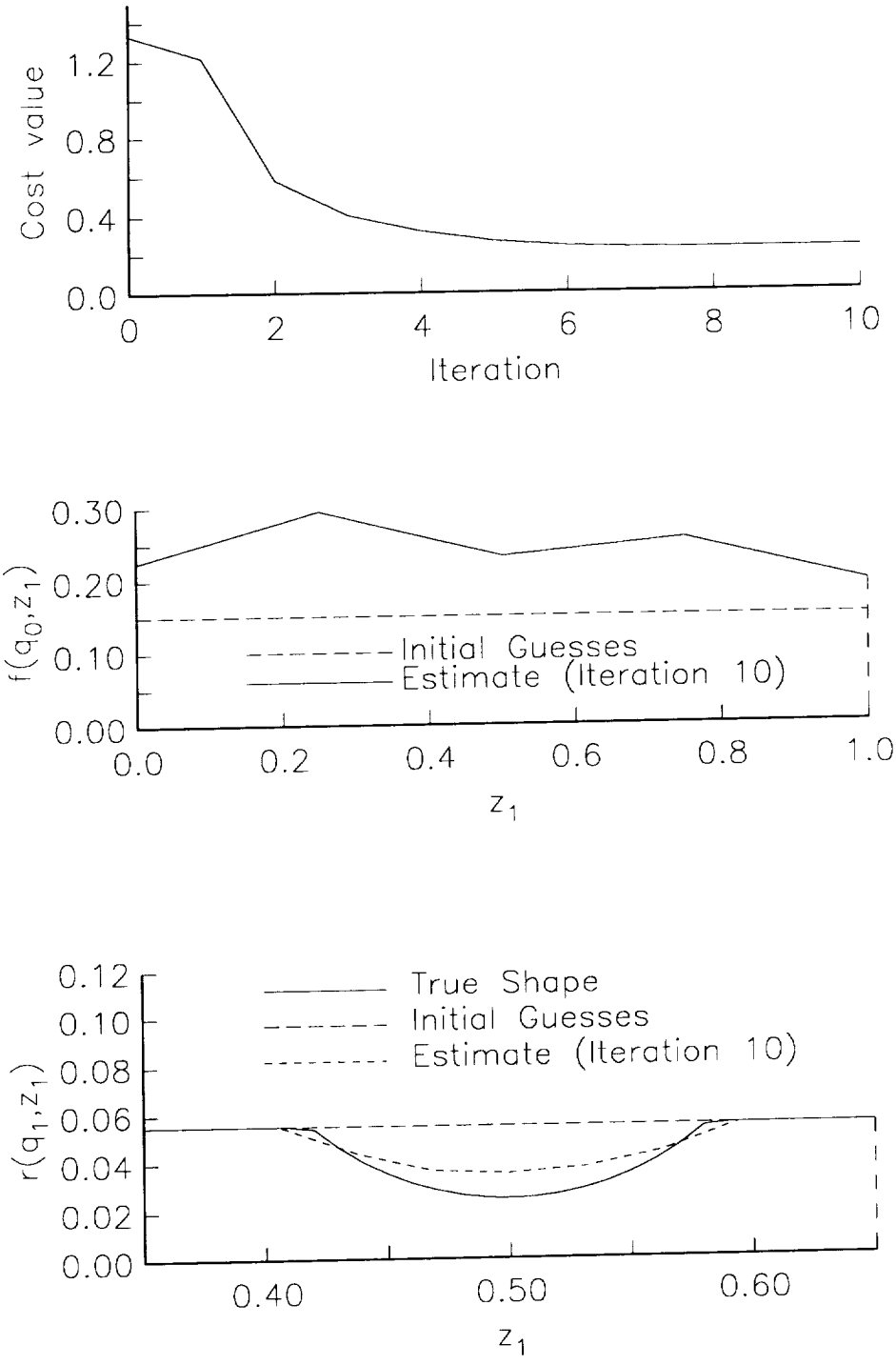

Figure 16. Estimated results (sample with corrosion)

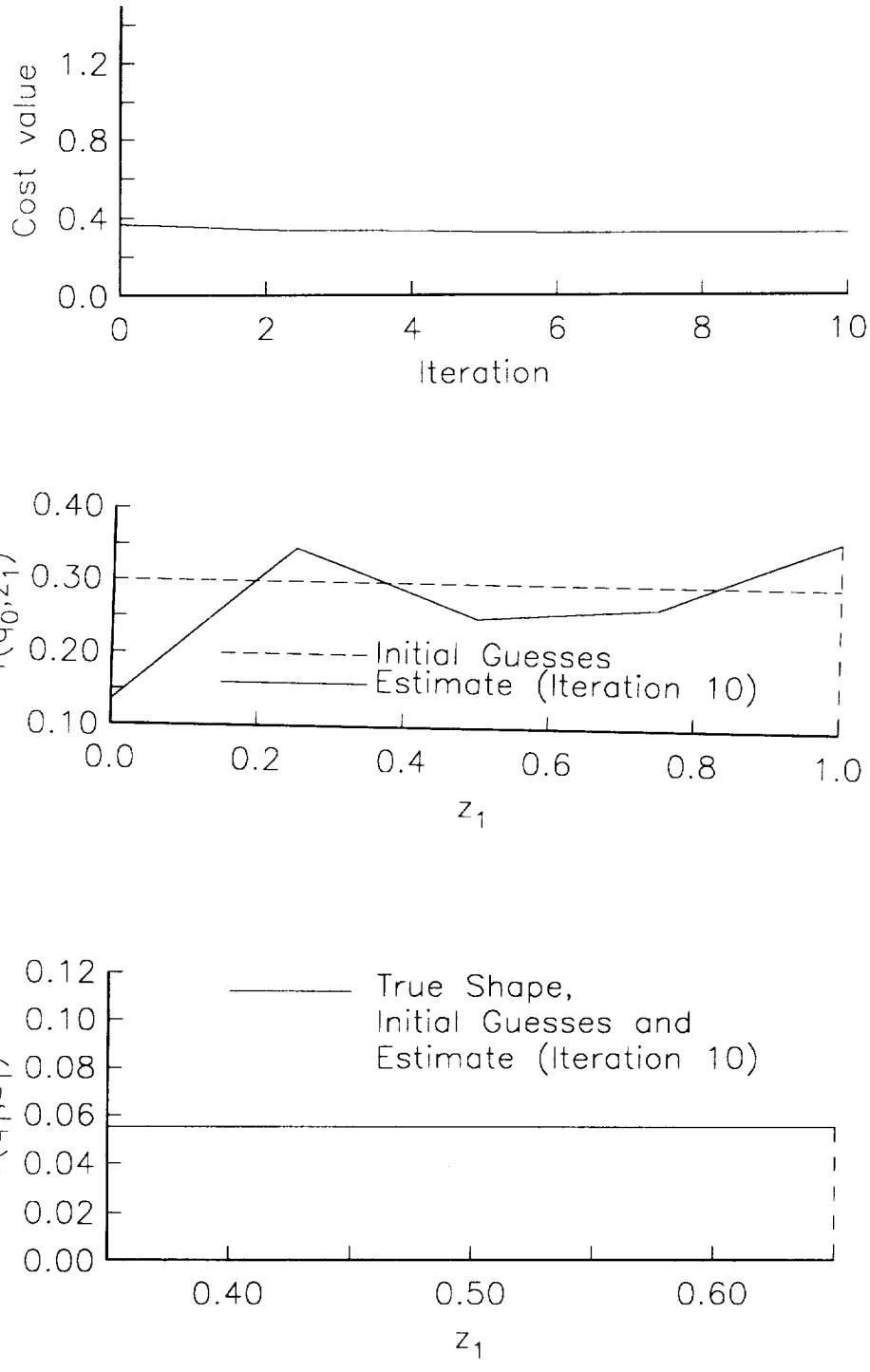

Figure 17. Estimated results (without corrosion)

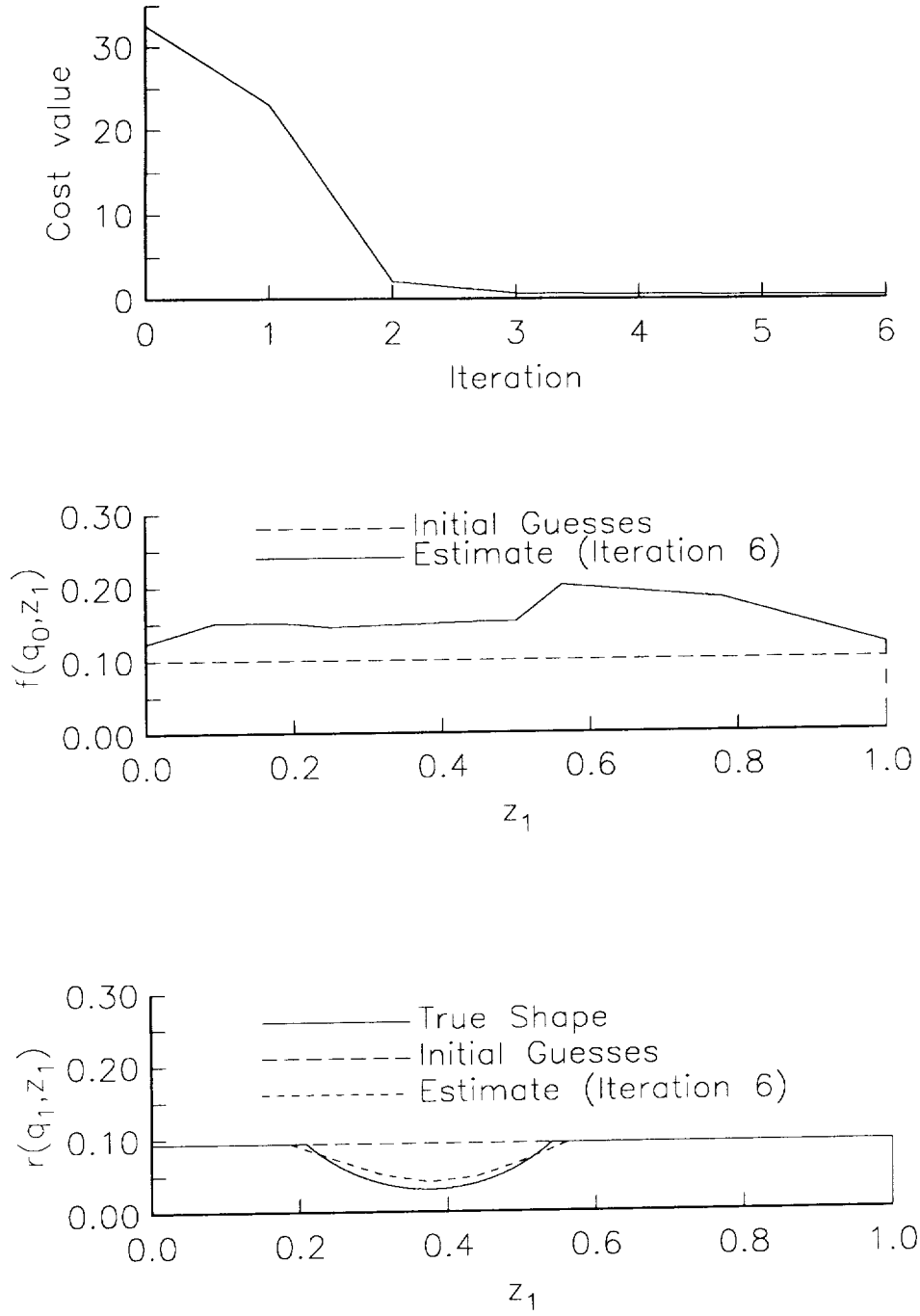

Figure 18. Estimated results (sample with corrosion)

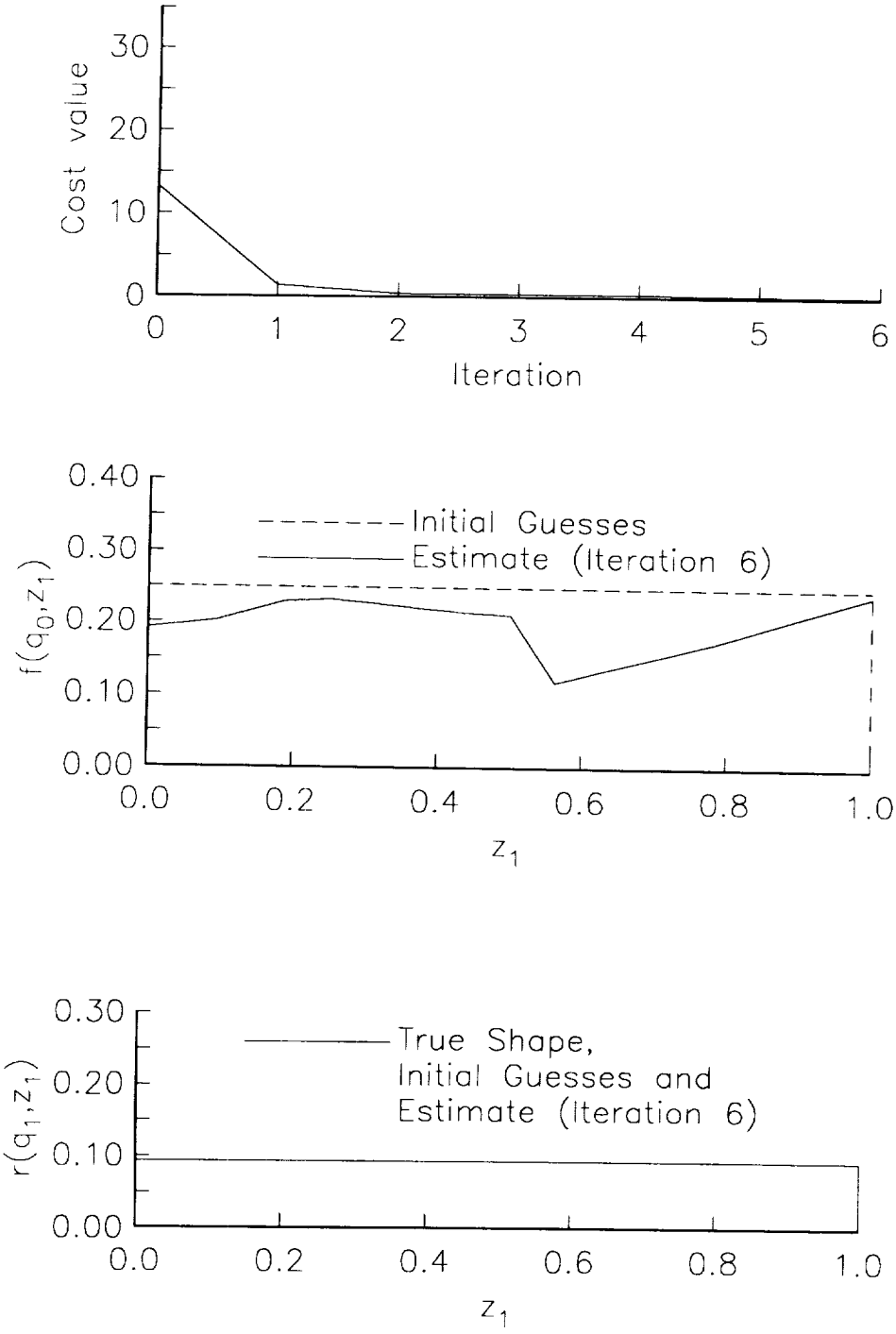

Figure 19. Estimated results (without corrosion)

The theoretical aspects of this paper can be quite properly considered as a nontrivial extension of the theory developed in [3], [4]. Here we present a very general theory employing the so-called "method of mappings" prominently used in optimal shape design problems (see [16] and [17]). The theory allows us to treat estimation of unknown boundary segments in quite general domains. These domains include as a special case (as is seen in Section IV) the types of domains treated in [3], [4]. While these more restrictive domains are precisely the ones needed to treat the experiments reported on in Section V, the theory of [3], [4] is not adequate for some of our current and ongoing investigations of material samples (with delaminations and holes). Moreover, in our theoretical formulation above we assume that the input flux as well as the boundary shape requires identification. This was done because we found it impossible to accurately measure the flux as well as the surface temperature in experiments with test samples. The theory of [3], [4], which assumes that the flux is given, is not adequate to treat the experimental examples discussed in Section V. Finally, the model used in [3], [4] includes a boundary transfer coefficient term as well as a radiative loss term in the heat equation. We found experimentally that both of these terms appear to be relatively unimportant so we have neglected them in the current model and theoretical development.

The theoretical developments above rely heavily on the framework given in [2]. Recently, Lamm has, in [12], developed an extension of the results in [2] which could also be used to treat the domain identification problems formulated in Sections I and II. The theory in [12] involves parameter dependent state spaces $H(p)$ as well as a fixed reference Hilbert space H. The example in Section 5 of [12] indicates how the theory developed there could be applied to problems involving unknown domains. Briefly, one has a parameterized domain Ω_p (analogous to our $G(q_1)$ above) and corresponding state spaces $H(p)$ where the norms in general also depend on the unknown parameters. The treatment of [12] involves heavy reliance on the properties of a "space-changing" map $\gamma(\tilde{p}, p) : H(p) \rightarrow H(\tilde{p})$ with $\gamma(\tilde{p}, p) = \gamma_t(\tilde{p})\gamma_e(p)$ where γ_e and γ_t are "extension" and "truncation" maps satisfying certain regularity conditions. (When applied to our problems, these are cordinate change maps.) In [12], the focus

is on the relationship between $H(p)$ and $H(\tilde{p})$ through the maps γ, γ_t and γ_e as opposed to one on the relationship between the parameter dependent spaces and a fixed reference space. The developments in [12] could offer some theoretical advantages (the computational procedures would still best be carried out as presented above in Sections III and IV) in that conditions (12), (13) and (14) of Theorem 1 above can be verified directly in the variable domain formulation of the problem. In this case one trades the tedium involving the coefficients of the transformed system (8), (9) above for some tedium involving changing (but equivalent) norms and verification of regularity properties for the "space-changing" maps (conditions related to (C-1)-(C-3) of our Theorem 1 above). We refer the interested reader to the example of Section 5 of [12] for details.

ACKNOWLEDGEMENTS

The authors gratefully acknowledge Mr. B. Scott Crews for his assistance in the experimental work described in this paper and Dr. R.G. Carter for his assistance and collaboration with regard to optimization software.

References

[1] O. Axelsson and V. A. Barker, Finite Element Solution of Boundary Value Problems, Academic Press, New York, 1984.

[2] H.T. Banks and K. Ito, "A unified framework for approximation in inverse problems for distributed parameter systems," Control-Theory Adv. Tech., Vol. 4 (1988), pp.73-90.

[3] H. T. Banks and F. Kojima, "Approximation techniques for domain identification in two-dimensional parabolic systems under boundary observations," Proc. 20th IEEE CDC Converence, Los Angeles, Dec. 9-11, (1987), pp. 1411-1416.

[4] H. T. Banks and F. Kojima, "Boundary shape identification problems in two-dimensional domains related to thermal testing of materials," Quart. Appl. Math., Vol. 47 (1989), pp. 273-293.

[5] D. Begis and R. Glowinski, "Application de la méthode des éléments finis á l'approximation d'un problème de domainde optimal. Méthodes de resolution des problèmes approchés," Appl. Math. Optim., Vol. 2 (1975), pp. 130-169.

[6] C. de Boor, A Practical Guide to Splines, Vol. 27, Applied Mathematical Science, Springer-Verlag, New York, 1978.

[7] R.G. Carter "Safeguarding Hessian approximations in trust region algorithms," Technical Report TR 87-12, Department of Mathematical Sciences, Rice University, 1987.

[8] D. Chanais, "On the existence of a solution in a domain identification problem," J. Math. Anal. Appl., Vol. 52 (1975), pp. 189-219.

[9] D. M. Heath, C. S. Welch, and W. P. Winfree, "Quantitative thermal diffusivity measurements of composites," in Review of Progress in Quantitative Nondestructive Evaluation, Plenum Publ., Vol. 5B (1986), pp. 1125-1132.

[10] F. Kojima, "Shape identification technique for a two-dimensional elliptic system by boundary integral equation method," ICASE Report No. 89-26, NASA Langley Research Center, Hampton, Virginia, April 1989.

[11] K. Kunish, "A review of some recent results on the output least squares formulation of parameter estimation problems," Automatica, Vol. 24 (1988), pp. 531-539.

[12] P. K. Lamm, "Parameter estimation for distributed equations in parameter-dependent state spaces:Applications to shape identification," to be submitted in SIAM J. Control & Optimization.

[13] J. L. Lions, Optimal Control of Systems Governed by Partial Differential Equations, Springer-Verlag, New York, 1971.

[14] J. J. Moré, "Recent developments in algorithms and software for trust region methods," in Mathematical Programming:The State of the Art (A. Bachem, M. Grötschel and B. Korte eds.), Springer-Verlag, New York, 1983.

[15] V.A. Morozov, Methods for Solving Incorrectly Posed Problems, Springer-Verlag, New York, 1984.

[16] F. Murat and J. Simon, "Studies on optimal shape design problems," in Lecture Notes in Computer Science, Vol. 41 (1976), pp.54-62, Springer-Verlag, New York.

[17] O. Pironneau, Optimal Shape Design for Elliptic Systems, Springer-Verlag, New York, 1983.

[18] J. Simon, "Differentiation with respect to the domain in boundary value problems," Numer. Funct. Anal. and Optim., Vol. 2, pp. 649-687, 1980.

NASA
National Aeronautics and Space Administration

Report Documentation Page

1. Report No.	2. Government Accession No.	3. Recipient's Catalog No.
NASA CR-181964 ICASE Report No. 89-44		

4. Title and Subtitle

BOUNDARY ESTIMATION PROBLEMS ARISING IN THERMAL TOMOGRAPHY

5. Report Date

November 1989

6. Performing Organization Code

7. Author(s)

H. T. Banks
Fumio Kojima
W. P. Winfree

8. Performing Organization Report No.

89-44

10. Work Unit No.

505-90-21-01

9. Performing Organization Name and Address

Institute for Computer Applications in Science and Engineering
Mail Stop 132C, NASA Langley Research Center
Hampton, VA 23665-5225

11. Contract or Grant No.

NAS1-18605

13. Type of Report and Period Covered

Contractor Report

12. Sponsoring Agency Name and Address

National Aeronautics and Space Administration
Langley Research Center
Hampton, VA 23665-5225

14. Sponsoring Agency Code

15. Supplementary Notes

Langley Technical Monitor:
Richard W. Barnwell

Final Report

Submitted to
Inverse Problems

16. Abstract

Problems on the identification of two dimensional spatial domains arising in the detection and characterization of structural flaws in materials are considered. For a thermal diffusion system with external boundary input, observations of the temperature on the surface are used in a output least square approach. Parameter estimation techniques based on the "method of mappings" are discussed and approximation schemes are developed based on a finite element Galerkin approach. Theoretical convergence results for computational techniques are given and the results are applied to experimental data for the identification of flaws in thermal testing of materials.

17. Key Words (Suggested by Author(s))	18. Distribution Statement
thermal tomography, parameter estimation, identification, partial differential equations	64 - Numerical Analysis 67 - Theoretical Mathematics Unclassified - Unlimited

19. Security Classif. (of this report)	20. Security Classif. (of this page)	21. No. of pages	22. Price
Unclassified	Unclassified	42	A03

NASA FORM 1626 OCT 86

NASA-Langley, 1990